Having confirmed that 1) **NC** could stabilize the duplex containing two contiguous T–G and G–G mismatches in **T1/C1** and 2) the T component was in the extrahelical position in the **NC**-bound TGG/CGG sequence, the binding of **NC** to the three contiguous mismatches T–G, G–G, and G–T in the TGG/TGG sequence was investigated. The 11-mers 5′-d(CCTTTGGTCAG)-3′ (**T2**) and 5′-d(CTGATGGAAGG)-3′ (**T3**) that had a 5′-TGG-3′ sequence were present as single-stranded forms at room temperature, as shown by the denaturation profile, because the possible duplex **T2/T3** should involve three contiguous mismatches (Figure 4a). At

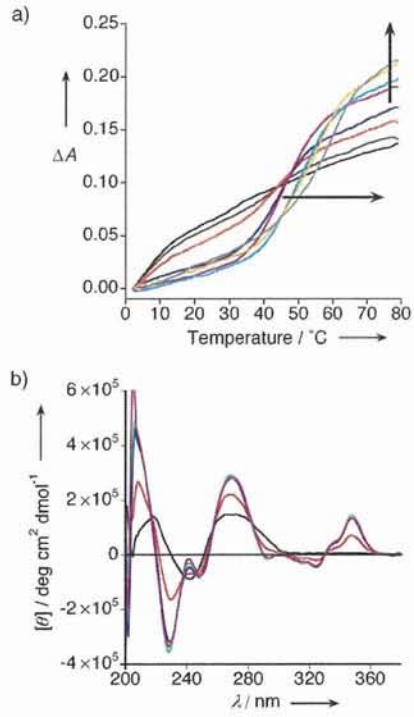

Figure 4. a) Thermal denaturation profile of **T2** and **T3** (5 μM each) with different concentrations of **NC** (0 (black), 2.5 (brown), 5 (red), 10 (blue), 20 (purple), 40 (cyan), 60 (yellow), and 100 μM (gray)). The vertical arrow indicates the increase in ΔA with increasing **NC** concentration. The horizontal arrow indicates the increase in melting temperature with increasing **NC** concentration. b) CD spectrum of **T2** and **T3** (5 μM each) measured in sodium cacodylate buffer (10 mM, pH 7.0) and NaCl (100 mM) at 25 °C in the absence (black) and presence of **NC** at 5 μM (red), 10 μM (blue), 15 μM (green), and 20 μM (purple).

increasing concentrations of **NC**, the transition from dsDNA to ssDNA became apparent and shifted toward a higher-temperature region. Notably, the T_m value for **T2** and **T3** reached 58.8 °C in the presence of 100 μM **NC**, thus showing the formation of a stable, **NC**-bound **T2/T3** duplex at room temperature.

The transition of ssDNA to dsDNA of **T2** and **T3** during titration with **NC** was monitored by circular dichroism (CD) spectroscopy (Figure 4b). Without **NC**, the CD spectrum of the mixture of **T2** and **T3** showed a positive band at 272 nm and a negative band at 250 nm. After addition of **NC**, the ellipticity of the positive band increased on increasing the amount of **NC** from one to four molar equivalents. In addition, the induced CD bands observed at 348 and 324 nm also changed their magnitude in response to the **NC** concentration. The change in CD involved the isodichroic points, and showed the transition of single-stranded **T2** and **T3** to the **NC**-bound duplex. The formation of the **NC**-bound duplex was further supported by CSI-TOF MS observations which indicated a 2:1 complex of **NC** with **T2/T3**. Again, the stoichiometry was exclusively 2:1. A selective strand cleavage of the 11-mer 5′-d(GCAATGGTTGC)-3′ (**T4**) at the T component in the TGG/TGG sequence was also confirmed by $KMnO_4$ oxidation upon binding of **NC** to the **T4/T4** duplex followed by heating with piperidine. In contrast, the protection of the other two T units from oxidation by $KMnO_4$ indicated that these components are in the intrahelical position (see Supporting Information).

The results described herein showed that **NC** could stabilize not only the two contiguous T–G and G–G mismatches in the TGG/CGG sequence, but also the three contiguous T–G, G–G, and G–T mismatches in the TGG/TGG sequence. By choosing an appropriate DNA sequence, two ssDNA molecules that do not spontaneously hybridize with each other could be adhered by the binding of **NC** to the TGG/TGG sequence. On the basis of **NC** binding to the CGG/CGG sequence, we used the TGG/TGG sequence in which the C component is substituted with another pyrimidine nucleotide base. In fact, the C component in the CGG/CGG sequence could be substituted with purine bases A and G, as evidenced by the CSI-TOF MS of the **NC**-bound complex for the AGG/AGG and GGG/GGG sequences. These results will be reported elsewhere. The molecule **NC** represents a new class of substances that function as molecular glue, not only in DNA hybridization but also in modulating the DNA secondary structure.

Received: March 25, 2006
Revised: May 26, 2006
Published online: July 21, 2006

Keywords: DNA · hybridization · mass spectrometry · nucleotides

[1] E. Winfree, F. Liu, L. A. Wenzler, N. C. Seeman, *Nature* **1998**, *394*, 539–544.
[2] B. Yurke, A. J. Turberfield, A. P. Mills, Jr., F. C. Simmel, J. E. Neumann, *Nature* **2000**, *406*, 605–608.
[3] H. Yan, S. H. Park, G. Finkelstein, J. H. Reif, T. H. LaBean, *Science* **2003**, *301*, 1882–1884.
[4] M. Endo, T. Majima, *Angew. Chem.* **2003**, *115*, 5922–5925; *Angew. Chem. Int. Ed.* **2003**, *42*, 5744–5747.
[5] S. Liao, N. C. Seeman, *Science* **2004**, *306*, 2072–2074.
[6] B. Ghosn, F. R. Haselton, K. R. Gee, W. T. Monroe, *Photochem. Photobiol.* **2005**, *81*, 953–959.
[7] H. Asanuma, T. Ito, T. Yoshida, X. Liang, M. Komiyama, *Angew. Chem.* **1999**, *111*, 2547–2549; *Angew. Chem. Int. Ed.* **1999**, *38*, 2393–2395.
[8] H. Asanuma, X. Liang, T. Yoshida, A. Yamazawa, M. Komiyama, *Angew. Chem.* **2000**, *112*, 1372–1374; *Angew. Chem. Int. Ed.* **2000**, *39*, 1316–1318.
[9] X. G. Liang, H. Asanuma, M. Komiyama, *J. Am. Chem. Soc.* **2002**, *124*, 1877–1883.

[10] K. Hamad-Schifferli, J. J. Schwartz, A. T. Santos, S. G. Zhang, J. M. Jacobson, *Nature* **2002**, *415*, 152–155.
[11] J. Yang, J. Y. Lee, H.-P. Too, G.-M. Chow, *Biophys. Chem.* **2006**, *120*, 87–95.
[12] T. Peng, K. Nakatani, *Angew. Chem.* **2005**, *117*, 7446–7449; *Angew. Chem. Int. Ed.* **2005**, *44*, 7280–7283.
[13] K. Nakatani, S. Hagihara, Y. Goto, A. Kobori, M. Hagihara, G. Hayashi, M. Kyo, M. Nomura, M. Mishima, C. Kojima, *Nat. Chem. Biol.* **2005**, *1*, 39–43.
[14] K. Yamaguchi, *J. Mass Spectrom.* **2003**, *38*, 473–490.
[15] H. Hayatsu, T. Ukita, *Biochem. Biophys. Res. Commun.* **1967**, *29*, 556–561.
[16] C. M. Rubin, C. W. Schmid, *Nucleic Acids Res.* **1980**, *8*, 4613–4620.
[17] A. M. Maxam, W. Gilbert, *Methods Enzymol.* **1980**, *65*, 499–560.
[18] J. A. Gogos, M. Karayiorgou, H. Aburatani, F. C. Kafatos, *Nucleic Acids Res.* **1990**, *18*, 6807–6814.

DOI: 10.1002/cbic.200600477

Detection of L-DNA-Tagged PCR Products by Surface Plasmon Resonance Imaging

Gosuke Hayashi,[a, b] Masaki Hagihara,[a, b] Akio Kobori,[a, c] and Kazuhiko Nakatani*[a, b]

Dedicated to Professor Isao Saito on the occasion of his 65th birthday.

The employment of tags plays an increasingly important role in genomics, in which PCR products are arrayed at the micro- or nanoscale. PCR products have been labeled in many ways. One conventional method is to incorporate labeled nucleotides into the PCR products during the extension reaction by DNA polymerase. Another method is to use a PCR primer that is labeled at the 5′ end. PCR primers with fluorophore labels are used for DNA sequencing, whereas biotinylated primers are used for the isolation and detection of the PCR products due to their strong and specific binding to streptavidin. Here, we report on a mirror-image DNA (L-DNA)-tagged PCR (LT-PCR) that enables us to label the PCR products with a defined sequence of L-DNA tag. The important findings leading to LT-PCR were that the L-DNA tag did not interfere with the PCR and remained as a single strand even after PCR. Therefore, LT-PCR products could be precisely delivered onto the DNA microarray, where the L-DNA complementary to the tag sequence was immobilized. A large number of sequences available for L-DNA tags would be suitable for such comprehensive microarray analysis. We demonstrated that the surface plasmon resonance imaging (SPR) array carrying the complementary L-DNA on the surface successfully detected the LT-PCR products without any purification or additional fluorescent labeling.

L-DNA consisting of L-2′-deoxyriboses is an enantiomer of natural DNA (D-DNA) and has unique properties.[1] L-DNA has been shown to be a poor substrate for the human *endo-* and *exo*-nucleases, as it has the opposite chirality to their intrinsic target,[2] and does not interact with single-stranded D-DNA, whereas it does bind sequence-selectively to complementary L-DNA. We anticipated that an L-DNA tag attached to a PCR primer at the 5′-end would not be recognized as a PCR template by DNA polymerase and would remain in a single-stranded form after amplification (Scheme 1). Besides L-DNA, a peptide nucleic acid (PNA) or D-DNA tag attached through a nonreplicable linker were conceivable for coding PCR products. However, the binding ability of PNA or D-DNA to complementary D-DNA might induce the formation of undesirable intraprimer hairpins or an interaction to an unexpected sequence of the template DNA. The intrinsic possibility of forming hairpin secondary structures and ambiguity in the effect on the PCR reactions thus makes them unsuitable for the labeling.

Primers used in LT-PCR consist of three parts, D-DNA to function as a general PCR primer, a L-DNA unit as a molecular tag, and three L-dTs as a spacer between the D and L-DNA. The spacer was inserted to mitigate steric congestion that might be produced between the left-handed and the right-handed duplexes upon hybridization of LT-PCR products with a complementary L-DNA. LT primers were synthesized by a conventional protocol of chemical DNA synthesis with phosphoramidites of D- and L-2′-deoxyribonucleosides. L-deoxynucleosides were synthesized according to the reported procedures.[3] Synthesized LT primers were purified by HPLC and PAGE, and identified by MALDI-TOF MS and enzymatic digestion experiments (see Figure S1 in the Supporting Information). The primers and oligonucleotides used in our study are shown in Table 1.

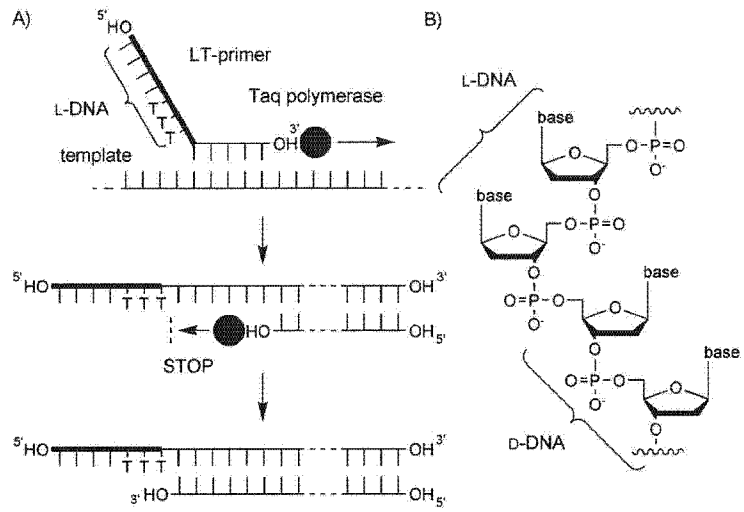

Scheme 1. An illustration of LT-PCR. A) The LT primer consists of an L-DNA sequence tag (thick line), a spacer of three L-dT nucleotides, and a D-DNA primer sequence (thin line). In the amplification reaction, DNA synthesis by Taq polymerase (●) stopped at the boundary between the L and D portions of the template. The products of LT-PCR contained a single-stranded L-DNA tag. B) Chemical structure at the boundary of D- and L-DNA in the LT primer.

LT-PCR with a primer set of L1-M13 and M13-RV was carried out with pUC18 plasmid as a template (Figure 1A). L1-M13 consisted of a 20-mer L-DNA tag, L-d(T)$_3$, and a 17-mer M13 forward primer sequence. The LT-PCR products obtained by L1-M13 and M13-RV showed slower migration on the nonde-

[a] G. Hayashi, Dr. M. Hagihara, Dr. A. Kobori, Prof. Dr. K. Nakatani
Department of Synthetic Chemistry and Biological Chemistry
Graduate School of Engineering, Kyoto University
Kyoto 615-8510 (Japan)

[b] G. Hayashi, Dr. M. Hagihara, Prof. Dr. K. Nakatani
Current address: Department of Regulatory Bioorganic Chemistry
The Institute of Scientific and Industrial Research, Osaka University
8–1 Mihogaoka, Ibaraki 567-0047 (Japan)
Fax: (+81) 6-6879-8459
E-mail: nakatani@sanken.osaka-u.ac.jp

[c] Dr. A. Kobori
Current address: Department of Biomolecular Engineering
Kyoto Institute of Technology (Japan)

Supporting information for this article is available on the WWW under http://www.chembiochem.org or from the author.

naturing PAGE analysis than 123 bp products obtained from a primer set of M13 and M13-RV (Figure 1B). The LT-PCR product showed two distinct bands in the denaturing PAGE analysis (Figure 1C). One band showed the same migration as that obtained by conventional PCR with a M13 primer set, whereas the other band showed slower migration. This result indicates that the LT-PCR products consisted of two DNA strands of different length. Since the migration of shorter DNA strand was almost the same as that of the PCR products produced from a M13 primer set, the DNA synthesis from the reverse primer M13-RV was most likely to stop around the boundary of D- and L-DNA on the template. The formation of two DNA strands of different length was also confirmed in LT-PCR carried out with a L2-GH and GH-RV primer set on pUC18 (Figure S2). The results were fully consistent with those obtained with a L1-M13 and M13-RV primer set.

Primer-extension experiments of 5′-FAM-labeled 13-mer (FAM13) further confirmed that Taq polymerase did not synthesize DNA on an L-DNA template (Figure S3). The product of the primer extension of FAM13 with an L1-M13 template was identified as FAM17 by denaturing PAGE analysis. MALDI-TOF MS also confirmed the formation of FAM17 but not any further elongated products, thus indicating that four nucleotides were added to the 3′-end of FAM13 on the template of D-DNA region but not a fifth. These results clarified that DNA synthesis by Taq polymerase on LT primer proceeded in the region of the D-DNA template but not in the region of the L-DNA template.

Table 1. Oligonucleotides used for our experiments.

Name	Sequence (5′ to 3′)[a]
L1-M13	^{L}(ATGCTACCGTATGCCCAGTGTTT)-^{D}(GTTTTCCCAGTCACGAC)
M13	^{D}(GTTTTCCCAGTCACGAC)
M13-RV	^{D}(CAGGAAACAGCTATGAC)
B-M13-RV	biotin-$(CH_2)_6$-^{D}(CAGGAAACAGCTATGAC)
L1C	^{L}(CACTGGGCATACGGTAGCAT)-$(CH_2)_6$-SH
L2C	^{L}(TTGGCTCTGTCTCCGTTGTC)-$(CH_2)_6$-SH

[a] Superscripts denote L- and D-DNA, respectively.

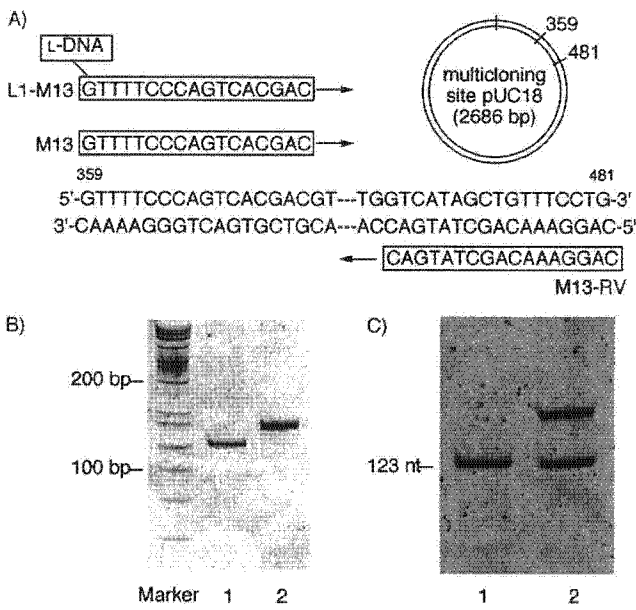

Figure 1. Analysis of LT-PCR products. A) Alignment of primers on pUC18. B) Native PAGE analysis of LT-PCR products obtained from a L1-M13 and M13-RV primer set (lane 2) and a 123 bp duplex obtained from a M13 and M13-RV primer set (lane 1). PCR products were loaded onto 10% polyacrylamide gel without any purification. Gel bands were stained by SYBR Green I. C) Denaturing PAGE analysis of the LT-PCR products. Lane 1, a PCR product from a M13 and M13-RV primer set; lane 2, a LT-PCR product obtained from a L1-M13 and M13-RV primer set. Gel bands were stained by SYBR Green II.

An identifiable L-DNA sequence tag that labeled the PCR products would be useful for isolating and detecting the desired PCR products in a duplex form. To demonstrate that the duplex form of the PCR products can be captured selectively at the designated position on the array surface, an SPR imaging array[4] carrying the complementary L-DNA to the L-DNA sequence tag was prepared. The 20-mer L-DNAs L1C and L2C, which were complementary to the L1 and L2 sequence tags, respectively, were synthesized with alkyl thiol modification at the 3′-end. L1C and L2C were immobilized onto the gold surface of sensor chips for the SPR imaging analysis (Figure 2A). After LT-PCR of pUC18 with two primer sets, each duplex of the LT-PCR products was separately applied onto the sensor surface without any purification procedures. When the LT-PCR products obtained from an L1-M13 and M13-RV primer set were applied to the SPR surface array, SPR signals were selectively detected on the L1C spots (Figure 2B), whereas distinct SPR signals were observed on the L2C spots when LT-PCR products obtained from a L2-GH and GH-RV primer set were applied (Figure 2C).

Under these experimental conditions, any L-DNA tagged primers that were not consumed in the PCR reaction should also bind to the complementary sequence on the array surface, because the PCR products were not purified prior to the array analyses. However, a sandwich assay with a secondary antibody clearly demonstrated that the observed SPR difference images were largely due to the binding of the duplex form of LT-PCR products on the SPR sensor surface. The assay exploited the 5′-biotinylated M13-RV (B-M13-RV) and L1-M13 for LT-PCR. The LT-PCR products were mixed with streptavidin (SA) and applied to the array surface. After complete hybridization of LT-PCR products, the successive addition of the antibody against SA to the surface resulted in a considerable increase in SPR intensity (Figure 2D). In contrast, virtually no signal increase was observed upon successive application of the mixture of L1-M13 and B-M13-RV without PCR and SA antibody (Figure 2E). These results proved that LT-PCR products could hybridize to complementary L-DNA immobilized on an array surface.

This report demonstrates that LT-PCR, a novel PCR technique, provides an efficient method for coding PCR products with a sequence-defined L-DNA tag. Without separation, purification, or denaturing–annealing processes, the products of LT-PCR could be captured in a duplex form on an SPR imaging surface array where L-DNA sequences complementary to tag sequences were immobilized. The LT-PCR and L-DNA SPR imaging array described here is just the first step in L-DNA tag technologies, which will be applicable to diverse molecular biology experiments.[5]

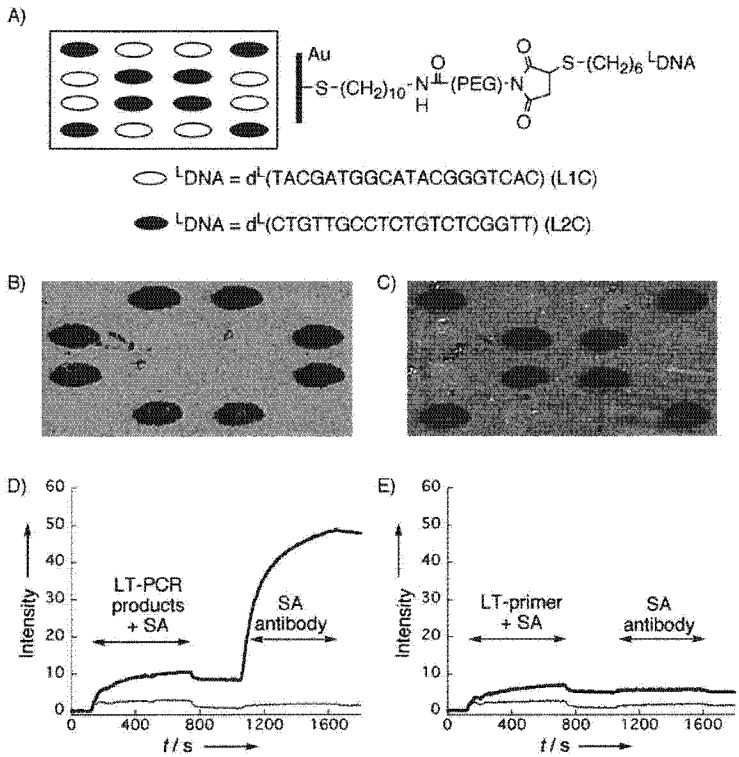

Figure 2. Detection of LT-PCR products on an L-DNA-immobilized SPR imaging array. A) Chemical structure of the L-DNA array surface and the immobilization pattern of L1C (○) and L2C (●). SPR difference images (between 30 and 600 s) obtained from LT-PCR products with B) a L1-M13 and M13-RV, and C) a L2-GH and GH-RV primer set. D) Sandwich assay with secondary antibody to SA. LT-PCR products obtained from a L1-M13 and B-M13-RV primer set were mixed with SA solution and applied to an L-DNA array. Significant interactions with the SA antibody were observed for the LT-PCR products. Key: signal at L1C, bold line; signal at the background spot, thin line. E) No interaction was observed for the solution without LT-PCR.

Experimental Section

LT-PCR: L-DNA-tagged PCR on pUC18 plasmid was performed with a primer set of L1-M13 and M13-RV, or of L2-GH and GH-RV. The amplification reaction was carried out with 500 nM of each primer, 1×Taq PCR Master Mix Kit (Qiagen), and pUC18 (100 pg μL^{-1}). The amplification protocol was 94 °C for 3 min; 35 cycles of 94 °C for 30 s, 55 °C for 30 s, and 72 °C for 1 min; and then 72 °C for 7 min. The LT-PCR products were analyzed by native PAGE (10% polyacrylamide gel, stained by SYBR Green I) and denaturing PAGE (8% polyacrylamide gel containing 7 M urea, stained by SYBR Green II).

Fabrication of the L-DNA-immobilized SPR imaging array: A gold-coated chip (SPR-200) for SPR imaging analysis was purchased from Toyobo (Japan). 8-Aminooctane-1-thiol (200 μL, 1 mM, Dojindo, Japan) in ethanol was dripped onto the gold surface and allowed to react for more than 7 h. After being washed with ethanol and distilled water, the aminoalkyl-modified surface was treated for 2 h with the heterobifunctional cross-linker MAL-PEG$_{12}$-NHS ester (200 μL, 5 mg mL^{-1}, Quanta Biodesign) to create a maleimido-modified surface. Drops of thiol-terminated L-DNA (10 nL, 20 μM) were delivered automatically onto the maleimido surface by using an automated spotter (Toyobo). The maleimido–thiol coupling was allowed to proceed overnight. The array surface was further treated with PEG-thiol (200 μL, 400 μg) for 2 h to block any remaining maleimido groups, then rinsed with a phosphate buffer and water. A phosphate buffer (10 mM phosphate, pH 7.2, 150 mM NaCl) was used for all array fabrication reactions.

SPR imaging analysis of LT-PCR products: The L-DNA-immobilized SPR array was placed in the SPR imager (Toyobo, Japan). After the surface had been washed with NaOH for 2 min, running phosphate buffer was applied to the array for 100 s, then LT-PCR products in the running buffer were applied for 5 min with a flow speed of 100 μL min^{-1}. Running buffer was then applied for a further 5 min. All SPR experiments were performed at 30 °C. The SPR array was reused after being washed with NaOH (0.5 M) for 3 min. The SPR images and signal data were collected with a MultiSPRinter Analysis program (Toyobo). The SPR difference images were constructed by using Scion Image (Scion, MD, USA).

Secondary antibody assay: LT-PCR was carried out with a primer set of L1-M13 and B-M13-RV. The product (40 μL) was mixed with a solution of streptavidin in phosphate buffer (90 μL 2 M) and applied onto the L1C-immobilized SPR surface array for 10 min. The array surface was further exposed to the SA antibody (20 μg mL^{-1}) for 10 min. For the negative control, the LT-PCR solution was analyzed by the same procedure without running the PCR amplification.

Acknowledgements

We are grateful to Toyobo Bio-laboratory for their instructions for SPR imaging experiments.

Keywords: chirality · DNA · polymerase chain reaction · surface plasmon resonance

[1] a) S. Fujimori, K. Shudo, Y. Hashimoto, *J. Am. Chem. Soc.* **1990**, *112*, 7436–7438; b) H. Urata, K. Shinohara, E. Ogura, Y. Ueda, M. Akagi, *J. Am. Chem. Soc.* **1991**, *113*, 8174–8175; c) M. Doi, M. Inoue, K. Tomoo, T. Ishida, Y. Ueda, M. Akagi, H. Urata, *J. Am. Chem. Soc.* **1993**, *115*, 10423–10433; d) A. Garbesi, B. L. Capobianco, F. P. Colonna, L. Tondelli, F. Arcamone, G. Manzini, C. W. Hilbers, J. M. E. Aelen, M. J. J. Blommers, *Nucleic Acids Res.* **1993**, *21*, 4159–4165; e) W. G. Purschke, F. Radtke, F. Keinjung, S. Klussmann, *Nucleic Acids Res.* **2003**, *31*, 3027–3032.

[2] K. P. Williams, X. Liu, T. N. M. Schumacher, H. Y. Lin, D. A. Ausiello, P. S. Kim, D. P. Bartel, *Proc. Natl. Acad. Sci. USA* **1997**, *94*, 11285–11290.

[3] a) H. Urata, E. Ogura, K. Shinohara, Y. Ueda, M. Akagi, *Nucleic Acids Res.* **1992**, *20*, 3325–3332; b) G. S. Ti, B. L. Gaffney, R. A. Jones, *J. Am. Chem. Soc.* **1982**, *104*, 1316–1319; c) Z. Shi, B. Yang, Y. Wu, *Tetrahedron* **2002**, *58*, 3287–3296.

[4] a) A. J. Thiel, A. G. Frutos, C. E. Jordan, R. M. Corn, L. M. Smith, *Anal. Chem.* **1997**, *69*, 4948–4956; b) K. Motoki, T. Yamamoto, H. Motohashi, T. Kamiya, T. Kuroita, T. Tanaka, J. D. Engel, B. Kawakami, M. Yamamoto, *Genes Cells* **2004**, *9*, 153–164; c) T. T. Goodrich, H. J. Lee, R. M. Corn, *J. Am. Chem. Soc.* **2004**, *126*, 4086–4087.

[5] Note added in proof. Independent work on the PCR with an L-DNA tag was recently reported. N. C. Hauser, R. Martinez, A. Jacob, S. Rupp, J. D. Hoheisel, S. Matysiak, *Nucleic Acids Res.* **2006**, *34*, 5101–5111.

Received: November 9, 2006
Published online on December 29, 2006

DOI: 10.1002/cbic.200700005

Bidirectional Control of Gold Nanoparticle Assembly by Turning On and Off DNA Hybridization with Thermally Degradable Molecular Glue

Tao Peng, Chikara Dohno, and Kazuhiko Nakatani*[a]

Hybridization of single-stranded DNA (ssDNA) with its complementary strand is important not only in many biological processes but also in DNA-based bioassays and nanodevices.[1–5] The high sequence specificity of hybridization has also been applied to the construction of nanometer-scale structures[6–8] and DNA-based molecular machines that include controlled motion of DNA.[9–11] Modulation and control of the formation of double-stranded DNA (dsDNA) is a general strategy for enhancing, limiting, or triggering these biological processes and functions. Several methods have been reported for the control of DNA hybridization by using photochemical[12–14] and electronic[15,16] reactions on chemically modified DNA. We have introduced the concept of "molecular glue" for the mediation of hybridization of unmodified DNA with synthetic small molecules that bind to sequences containing up to three contiguous base mismatches. Molecular glue can adhere to two unmodified ssDNA molecules that do not hybridize with each other.[17,18] The function of the molecular glue that we previously reported relied on thermodynamically favorable ligand binding to two ssDNA molecules.[17] Its function did not include the denaturation of the duplex once formed, and was limited to the unidirectional control of DNA hybridization. To achieve bidirectional control, that is, to turn DNA hybridization on and off, we have looked for methods to inactivate the molecular glue in the reaction system. Here, we describe bidirectional control of DNA hybridization by using the new thermally degradable molecular glue, TD (Scheme 1). Irreversible thermal conversion of TD into its inactive form allowed us to control the DNA hybridization/denaturation cycle. This method for turning DNA hybridization on and off was then applied to the control of the assembly of gold nanoparticles.

TD consists of two naphthyridine heterocycles that recognize guanine and selectively bind to dsDNA molecules with G–G mismatches. A key feature of TD, compared to the molecular glue previously reported, is its ability to function as a glue for DNA at room temperature but then be inactivated at an elevated temperature. In order to acquire inactivation, we modified the structure of the original molecule and found that, at an elevated temperature, the bond that connects the two naphthyridine heterocycles can be removed, which remarkably results in the inactivation of the glue function.[19] Thermolysis of TD in 10 mM sodium cacodylate buffer (pH 7.0), as monitored by reversed-phase HPLC, showed that TD was completely consumed within 4 min incubation at 80 °C with concomitant formation of two products (Figure 1). The products were identified as 2-amino-7-methyl-1,8-naphthyridine (**1**) and (7-methyl-1,8-naphthyridin-2-yl)-carbamic acid 2-(2-oxo-oxazolidin-3-yl)-ethyl ester (**2**; Figure 1B). The formation of **1** and **2** indicated that TD underwent thermal fragmentation by an intramolecular carbamate exchange. These results showed that TD could be irreversibly transformed to **1** and **2** by simple heating, and was therefore no longer effective in stabilizing dsDNA.

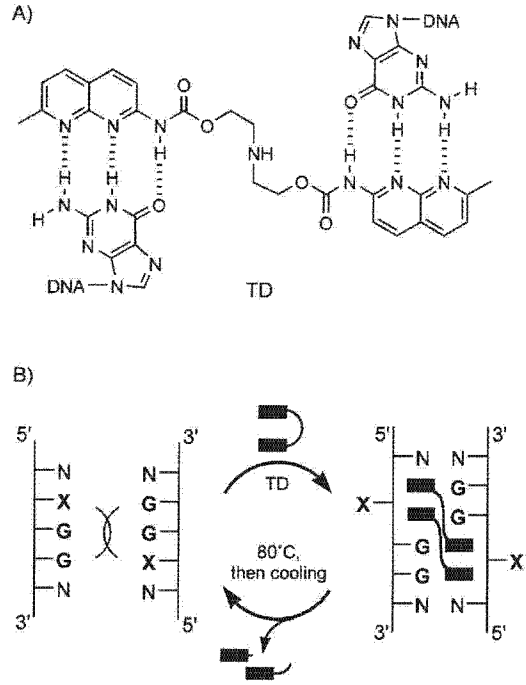

Scheme 1. A) The structure of TD and its hydrogen-bonding pattern with guanines on opposing strands of a DNA duplex. B) Schematic representation of TD-assisted hybridization of two ssDNA molecules that contain the sequences 5′-XGG and 5′-XGG (X = C or T), and denaturation of TD-bound dsDNA by heat-induced inactivation of TD followed by gradual cooling to room temperature. The X bases in the XGG/XGG sequence are expected to be flipped-out of the helix, as shown on the right-hand side of the arrow.

The function of TD as a molecular glue for DNA was confirmed by measuring the melting temperature (T_m) of 11-mer duplexes (5′-d(CTA ACX GAA TG)-3′/5′-d(CAT TCY GTT AG)-3′) that contained mismatches. Experiments were carried out with all possible combinations of matched and mismatched base pairs (represented by X–Y in the sequences) in the absence and presence of TD. TD selectively bound to the dsDNA that contained the G–G mismatch (X = Y = G; see the Supporting Information). In the presence of 100 μM TD, the T_m increase (ΔT_m) for the duplex that contained the G–G mismatch was 25.7 °C;

[a] *Dr. T. Peng, Dr. C. Dohno, Prof. K. Nakatani*
Department of Regulatory Bioorganic Chemistry
The Institute of Scientific and Industrial Research (SANKEN)
Osaka University
8–1 Mihogaoka, Ibaraki 567-0047 (Japan)
Fax: (+81) 6-6879-8459
E-mail: nakatani@sanken.osaka-u.ac.jp

Supporting information for this article is available on the WWW under http://www.chembiochem.org or from the author.

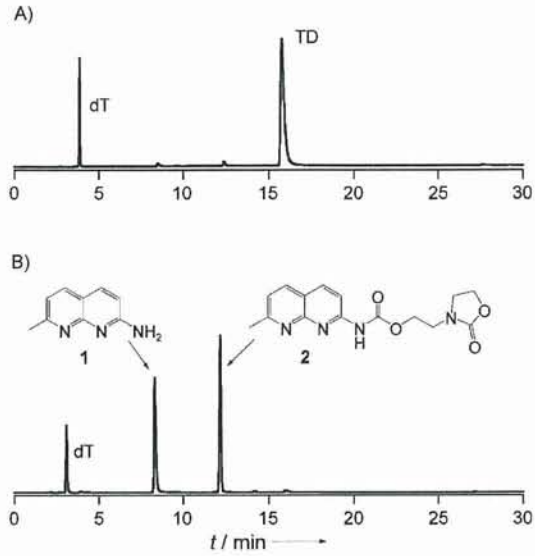

Figure 1. HPLC profiles for the thermolysis of TD (0.71 mM) in sodium cacodylate buffer (10 mM, pH 7.0). A) Before, and B) after heating at 80 °C for 4 min; deoxythymidine (dT) was added as an internal standard. After heating, TD underwent irreversible thermal fragmentation to form products **1** and **2**.

this is comparable with results obtained for the previous version of the molecular glue.[17] Since the cytosines in the CGG/CGG duplex are expected to be flipped out of the helix[18,20] (Scheme 1 B) they can be substituted with other bases in order to either decrease or increase the T_m of the oligonucleotides.[17] Indeed, the ΔT_m value reached more than 30 °C (T_m = 54.0 °C) for the 11-mer duplex 5′-d(CCTTTGGTCAG)-3′/5′-d(CTGACGGAAGG)-3′, which includes two contiguous T–G and G–G mismatches (Figure 2 A). TD markedly stabilized the mismatch-containing duplex, and apparently acted as molecular glue for DNA at room temperature. The function of TD, however, could be completely terminated by simple heating. After heating the TD-bound TGG/CGG mismatch-containing duplex at 80 °C for 5 min the T_m value decreased back to the original value for this molecule (Figure 2 A). The marked change in duplex stability can be rationalized by quantitative and irreversible transformation of TD into the inactive form by heating. The transition between ssDNA and TD-bound dsDNA was clearly observed in the CD spectra (Figure 2 B). In the presence of TD, the CD spectrum of TGG/CGG mismatch-containing oligonucleotide was significantly different from the sample without TD. After heating the TD-containing sample at 80 °C for 5 min and subsequent gradual cooling to room temperature, its CD spectrum was virtually identical to that of the sample that did not contain TD.

DNA-functionalized gold nanoparticles have been intensively used for many applications, including the construction of nanostructures, biosensor, and diagnostic tools.[4,21] Reversible assembly/disassembly of gold nanoparticles has been achieved by the use of DNA or protons as fuel.[22,23] The transformation between ssDNA and TD-bound dsDNA shown above, was used to control the assembly of gold nanoparticles. Gold nanoparticles 15 nm in diameter were functionalized with DNA through

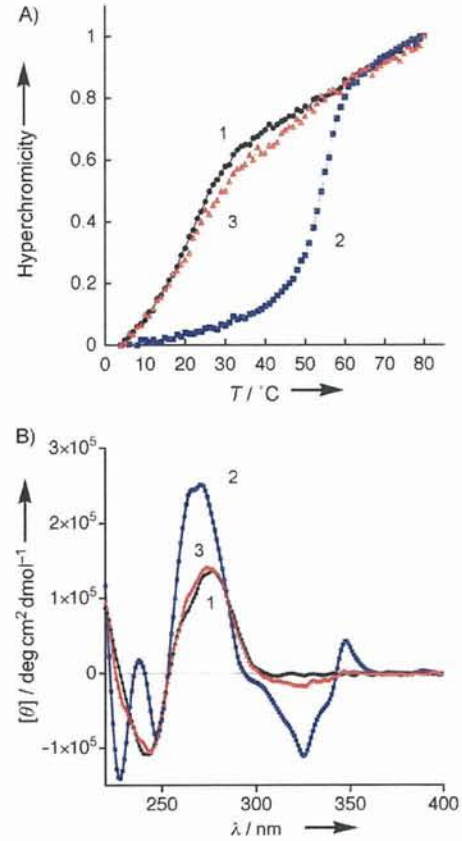

Figure 2. TD-assisted hybridization and denaturation. A) Thermal UV-melting curves were measured for duplex 5′-d(CCTTTGGTCAG)-3′/5′-d(CTGACGGAAGG)-3′ (4.5 μM) in sodium cacodylate buffer (10 mM, pH 7.0) containing NaCl (0.1 M). The temperature was increased from 4 to 80 °C at a rate of 1 °C min^{-1}. Sample 1: DNA only (●, T_m = 21 °C); sample 2: DNA with TD (100 μM; ■, T_m = 54 °C); sample 3: DNA with TD (100 μM) after being heated at 80 °C for 5 min and then gradually cooled to room temperature (▲, T_m = 21 °C). B) CD spectra of the same samples used for melting curve measurements.

a 5′-thiol-modified A_{20} spacer, and two sets of DNA-modified gold nanoparticles, NP1 and NP2, were prepared (Figure 3 A).[21] The DNA sequences attached to NP1 and NP2 were hybridized with the linker DNA oligonucleotides L1 and L2, respectively. This resulted in the 5′-heptamer overhangs 5′-TTCGGTT-3′ and 5′-AATGGAA-3′ on L1 and L2, respectively. These overhangs contained the TD-binding site CGG/TGG. In the absence of TD, formation of the L1–L2 duplex by hybridization was not favored due to two contiguous T–G and G–G mismatches. As a result, the gold nanoparticles, NP1 and NP2, were dispersed in solution and therefore exhibited a red color due to plasmon absorption (Figure 3 B, state 1). In the presence of TD, plasmon absorption was red-shifted from 522 to 532 nm and the intensity decreased; this indicated the aggregation of the gold nanoparticles (Figure 3 B and C, state 2).[4,21–23] The molecular glue, TD, brought the overhang sequences in L1 and L2 together to form the TD-bound L1–L2 duplex, and assembled the NP1 and NP2 nanoparticles attached to the dsDNA. The aggregation of NP1 and NP2 particles was therefore propagated by their being coated with multiple DNA molecules. In

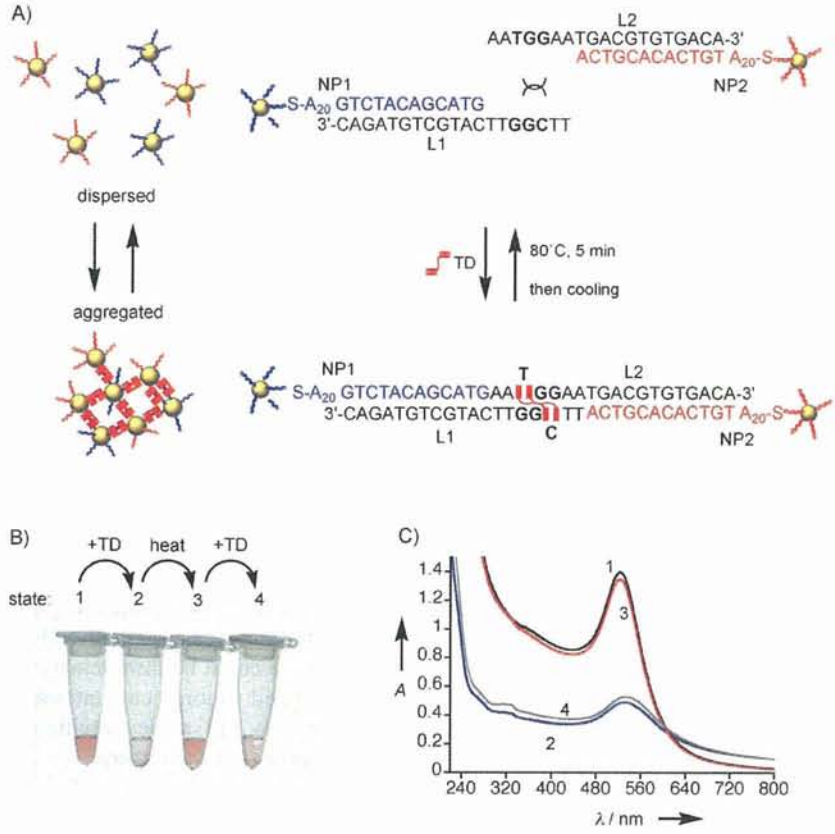

Figure 3. Control of gold nanoparticle assembly by using TD-assisted hybridization and denaturation. A) Illustration of nanoparticle assembly: the 5'-overhang heptamers on L1 and L2 contained the TD-binding CGG/TGG sequence (bold). Upon binding of TD to this sequence, the gold nanoparticles, NP1 and NP2, were assembled. After being heated at 80 °C for 5 min, TD was inactivated; this led to the disassembly of NP1 and NP2 aggregates. B) Colorimetric assay for nanoparticle aggregation in response to the function of TD: state 1, NP1 + NP2 + L1 + L2; state 2, NP1 + NP2 + L1 + L2 + TD; state 3, after heating state 2 solution at 80 °C for 5 min and gradual cooling to room temperature; state 4, TD + state 3 solution. C) UV-visible spectra of solutions of states 1–4.

marked contrast to the assembly of gold nanoparticles by using conventional DNA hybridization, particles aggregated through TD-binding could again be dispersed simply by heating the solution at 80 °C for 5 min (Figure 3 B, state 3). The red color of the solution persisted at room temperature. This clearly indicates that heating caused inactivation of TD and conversion of the TD-bound L1–L2 duplex to single strands, and therefore the dispersion of NP1 and NP2. Upon addition of TD to the redispersed particles, aggregation took place again (Figure 3 B, state 4). The changes in the plasmon absorption band from state 1 through to state 4 were monitored by UV-visible spectra, and were fully consistent with the assembly of gold nanoparticles in response to TD-assisted hybridization and denaturation of L1 and L2 (Figure 3 C).

In summary, we have developed a new DNA molecular glue, TD, which allows bidirectional control of hybridization of unmodified DNA. This was demonstrated by the assembly and disassembly of gold nanoparticles. Bidirectional control of DNA hybridization will be applicable to DNA-based construction of nanostructures and -machines. Control of DNA hybridization by a small molecule provides a new strategy for constructing programmable DNA-based nanomaterials.

Acknowledgements

This work was supported by Grant in Aid for Scientific Research (S) from the Japan Society for the Promotion of Science.

Keywords: DNA · gold · hybridization · mismatches · nanoparticles

[1] N. C. Seeman, *Nature* **2003**, *421*, 427–431.
[2] J. G. Hacia, *Nat. Genet.* **1999**, *21*, 42–47.
[3] Y. Ito, E. Fukusaki, *J. Mol. Catal. B Enzym.* **2004**, *28*, 155–166.
[4] N. L. Rosi, C. A. Mirkin, *Chem. Rev.* **2005**, *105*, 1547–1562.
[5] E. Katz, I. Willner, *Angew. Chem.* **2004**, *116*, 6166–6235; *Angew. Chem. Int. Ed.* **2004**, *43*, 6042–6108.
[6] U. Feldkamp, C. M. Niemeyer, *Angew. Chem.* **2006**, *118*, 1888–1910; *Angew. Chem. Int. Ed.* **2006**, *45*, 1856–1876.
[7] Z. Deng, S.-H. Lee, C. Mao, *J. Nanosci. Nanotechnol.* **2005**, *5*, 1954–1963.
[8] K. V. Gothelf, T. H. LaBean, *Org. Biomol. Chem.* **2005**, *3*, 4023–4037.
[9] B. Yurke, A. J. Turberfield, A. P. Mills, Jr., F. C. Simmel, J. E. Neumann, *Nature* **2000**, *406*, 605–608.
[10] H. Yan, X. Zhang, Z. Shen, N. C. Seeman, *Nature* **2002**, *415*, 62–65.
[11] J. S. Shin, N. A. Pierce, *J. Am. Chem. Soc.* **2004**, *126*, 10834–10835.
[12] H. Asanuma, T. Ito, T. Yoshida, X. Liang, M. Komiyama, *Angew. Chem.* **1999**, *111*, 2547–2549; *Angew. Chem. Int. Ed.* **1999**, *38*, 2393–2395.
[13] H. Asanuma, X. Liang, T. Yoshida, M. Komiyama, *ChemBioChem* **2001**, *2*, 39–44.
[14] B. Ghosn, F. R. Haselton, K. R. Gee, W. T. Monroe, *Photochem. Photobiol.* **2005**, *81*, 953–959.
[15] K. Hamad-Schifferli, J. J. Schwartz, A. T. Santos, S. G. Zhang, J. M. Jacobson, *Nature* **2002**, *415*, 152–155.
[16] J. Yang, J. Y. Lee, H.-P. Too, G.-M. Chow, *Biophys. Chem.* **2006**, *120*, 87–95.
[17] T. Peng, C. Dohno, K. Nakatani, *Angew. Chem.* **2006**, *118*, 5751–5754; *Angew. Chem. Int. Ed.* **2006**, *45*, 5623–5623.
[18] T. Peng, K. Nakatani, *Angew. Chem.* **2005**, *117*, 7446–7449; *Angew. Chem. Int. Ed.* **2005**, *44*, 7280–7283.
[19] T. Peng, T. Murase, Y. Goto, A. Kobori, K. Nakatani, *Bioorg. Med. Chem. Lett.* **2005**, *15*, 259–262.
[20] K. Nakatani, S. Hagihara, Y. Goto, A. Kobori, M. Hagihara, G. Hayashi, M. Kyo, M. Nomura, M. Mishima, C. Kojima, *Nat. Chem. Biol.* **2005**, *1*, 39–43.
[21] J. J. Storhoff, R. Elghanian, R. C. Mucic, C. A. Mirkin, R. L. Letsinger, *J. Am. Chem. Soc.* **1998**, *120*, 1959–1964.
[22] P. Hazarika, B. Ceyhan, C. M. Niemeyer, *Angew. Chem.* **2004**, *116*, 6631–6633; *Angew. Chem. Int. Ed.* **2004**, *43*, 6469–6471.
[23] Y. H. Jung, K.-B. Lee, Y.-G. Kim, I. S. Choi, *Angew. Chem.* **2006**, *118*, 6106–6109; *Angew. Chem. Int. Ed.* **2006**, *45*, 5960–5963.

Received: January 4, 2007
Published online on February 15, 2007

DOI: 10.1002/chem.200601496

Allele Specific C-Bulge Probes with One Unique Fluorescent Molecule Discriminate the Single Nucleotide Polymorphism in DNA

Fumie Takei,[a] Hitoshi Suda,[b] Masaki Hagihara,[a] Jinhua Zhang,[a] Akio Kobori,[b] and Kazuhiko Nakatani*[a, b]

Abstract: A combination of an allele specific C-bulge probe and the fluorescent molecule *N,N'*-bis(3-aminopropyl)-2,7-diamino-1,8-naphthyridine (DANP) that binds specifically to the C-bulge provides a method for single nucleotide polymorphism (SNP) typing with only one fluorescent molecule without covalent modification of the DNA probe. The allele specific C-bulge probe contains one additional cytosine and produces a C-bulge directly flanking the SNP site upon hybridization to the target DNA. The C-bulge is a scaffold to recruit and retain DANP directly neighboring the SNP site. The DANP fluorescent probe was selectively modulated by the flanking matched and mismatched base pairs. The mutation type could be discriminated by the modulated fluorescent intensity with respect to the allele specific C-bulge probes used for the assay.

Keywords: cytosine bulge · DNA recognition · fluorescent probes · mutation detection

Introduction

Typing of the single nucleotide polymorphisms (SNPs) in an individual genome against sets of predetermined disease-related SNPs is essential to achieve personalized medicine.[1–6] Besides methods which exploit the sequence-specific reactions of enzymes,[1–4] the challenge toward novel SNP typing methods based on organic chemistry draws attention to molecular systems that emit fluorescence in an allele specific manner.[7–19] Base discrimination by fluorescent molecules largely relies on the change in the fluorescent intensity upon formation of the matched or mismatched base pair. The chemical basis of the fluorescence change is a result of the modulation of the dielectric and hydrogen-bonding environments of the fluorescent chromophore. To exert the maximum influence of the base pairing on the fluorescence intensity, the fluorescent molecules have thus been developed near the SNP site by covalently linking the probe DNA and/or directly bind to the base at the SNP site.[7,15–19] In the latter strategy, the use of four fluorescent molecules selectively responding to each one of the four nucleotide bases has been investigated.[15–19]

In terms of convenience and simplicity of the assay, typing methods using fluorescent molecules would be particularly effective if the covalent modification of the probe DNA were not required, and if all four nucleotide bases could be analyzed by one unique fluorescent molecule. To address these issues, we have investigated a method exploiting allele specific C-bulge probe DNA and a fluorescent molecule selectively binding to the C-bulge. The C-bulge probe DNA is allele specific by alternating the nucleotide base (^{Y}N) opposite the SNP site (^{X}N) and contains one additional cytosine directly neighboring ^{Y}N. The probe DNA provides a C-bulge as a scaffold to recruit and keep the fluorescent molecule directly neighboring the SNP site (Figure 1). We have reported that *N,N'*-bis(3-aminopropyl)-2,7-diamino-1,8-naphthyridine (DANP) selectively and strongly bound to the C-bulge with an exclusive 1:1 stoichiometry.[20] DANP binds to the C-bulge as the protonated form DANPH$^+$ at a neutral pH (Figure 2). Therefore, DANP would be recruited to the cytosine bulge that is located directly adjacent to the matched or mismatched base pair ^{X}N–^{Y}N at the SNP site. DANPH$^+$ emitted characteristic fluorescence upon binding to the cytosine bulge. Upon binding, both absorption and emission maximum of DANPH$^+$ were shifted by 30 nm to a longer wavelength from those of the unbound DANP. Therefore, it is possible to selectively monitor the DANPH$^+$

[a] Dr. F. Takei, Dr. M. Hagihara, Dr. J. Zhang, Prof. K. Nakatani
Department of Regulatory Bioorganic Chemistry
The Institute of Scientific and Industrial Research
Osaka University, 8-1 Mihogaoka, Ibaraki 567-0047 (Japan)
Fax: (+81) 6-6879-8459
E-mail: nakatani@sanken.osaka-u.ac.jp

[b] H. Suda, Dr. A. Kobori, Prof. K. Nakatani
Department Synthetic Chemistry and Biological Chemistry
Kyoto University, Nishigyou-ku, Kyoto 615-8510 (Japan)

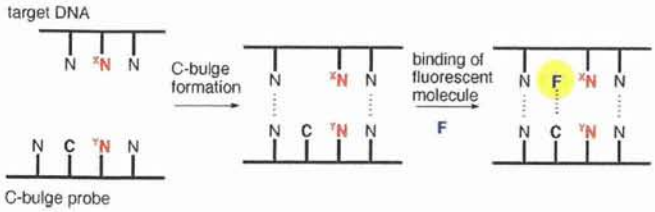

Figure 1. Illustration of the SNP typing exploiting the C-bulge binding molecule DANP and C-bulge probe as a scaffold to recruit DANP to the region directly neighbouring the SNP site. ^{X}N: nucleotide to be determined at the SNP site; ^{Y}N: nucleotide opposite ^{X}N in the probe; C: the bulged cytosine; F: fluorescent molecule binding to C-bulge (DANP).

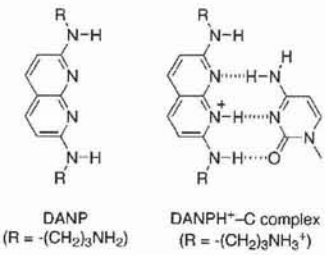

Figure 2. Structures of DANP and DANPH$^+$–C complex.

bound to the C-bulge even in the presence of unbound DANP.

The feasibility of the proposed method depends entirely on 1) the DANPH$^+$ is bound to the C-bulge flanking the mismatched base pair and 2) the DANPH$^+$ fluorescence could be modulated by the neighboring base pair. We have investigated the binding of DANP to the C-bulge flanking the mismatched base pairs and the fluorescence behavior upon binding. We report here that the fluorescence of the DANPH$^+$ bound to the C-bulge was, in fact, selectively modulated by the neighboring matched or mismatched base-pair formation. The profile in the fluorescence change of DANPH$^+$ regarding the allele specific C-bulge probes may be used for the determination of the allele type at the predetermined SNP site.

Results and Discussion

First we looked at the DANPH$^+$ binding to the C-bulge flanking the mismatched base pairs. The formation of the DANPH$^+$-bound complex was investigated by measuring the melting temperature (T_m) of the 16-mer target DNA 5′-d(ACATCCAA^{X}NCAACCAC)-3′ and 17-mer C-bulge probes 5′-d(GTGGTTG^{Y}NCTTGGATGT)-3′ in the presence of DANP. The C-bulge probes contained one additional cytosine (italic) flanking ^{Y}N (N = A, T, C, G, and I) opposite ^{X}N. We have used inosine (I) in addition to A, T, C, and G to avoid the fluorescence quenching by G in the C-bulge probe. Upon hybridization, a single C-bulge was produced directly neighboring the ^{X}N–^{Y}N base pair. By alternating ^{Y}N with A, T, G, C, and I with respect to four ^{X}N in the target DNA, C-bulge duplexes flanking 20 different matched and mismatched base pairs were produced. The T_m of the duplex contained ^{X}T, ^{X}A, and ^{X}C increased in the presence of DANP regardless to the base at ^{Y}N (Table 1). Based on the

Table 1. Melting temperatures of C-bulge duplexes with DANP.[a]

	5′-d(ACATCCAA_^{X}NCAACCAC)-3′ 3′-d(TGTAGGTTC^{Y}NGTTGGTG)-5′			
^{Y}N	^{X}T	^{X}A	^{X}G	^{X}C
A	52.2 (4.8)[b]	46.7 (2.7)	52.2 (0.6)	46.3 (3.9)
T	47.3 (5.3)	50.4 (3.2)	53.5 (1.0)	46.6 (5.0)
C	48.1 (5.5)	46.7 (4.0)	56.0 (2.3)	48.1 (6.7)
G	50.3 (6.0)	51.8 (2.9)	54.3 (1.1)	54.6 (3.6)
I	48.2 (5.5)	52.2 (4.2)	52.5 (0.5)	49.4 (3.1)

[a] T_m of duplexes 5′-d(ACATCCAA^{X}NCAACCAC)-3′/5′-(GTGGTTG^{Y}NCTTGGATGT)-3′ (2 μM) were measured in 10 mM Na cacodylate (pH 7.0) with 100 mM NaCl in the presence of DANP (50 μM). [b] The values in a parenthesis refer to the increase of T_m compared with the values measured without DANP. The reported values are the average of three independent measurements.

K_d value of 10 mM for the DANPH$^+$ binding to the C-bulge,[20] it was estimated that about 80% of the C-bulge duplex was present as the DANPH$^+$-bound form under these conditions. Duplexes containing ^{X}G showed much smaller increases of T_m than other duplexes especially when ^{Y}N was A, T, G, and I. This is probably due to the unavoidable formation of ^{X}G–C base pair between ^{X}G and the extra cytosine, producing a single ^{Y}N bulge instead of the C-bulge.

Having confirmed the binding of DANP to the C-bulge flanking the ^{X}T–^{Y}N, ^{X}A–^{Y}N, and ^{X}C–^{Y}N base pairs, we focused our attention on the fluorescence of the DANPH$^+$ bound to the C-bulge. The fluorescence measurements were performed in the presence of an excess amount of C-bulge duplex to make sure that DANP was completely bound to the C-bulge. The DANPH$^+$ fluorescence was selectively modulated by the base pairs flanking the C-bulge (Figure 3). Strong fluorescence was observed when the base pair flanking the C-bulge was ^{X}A–^{Y}T, whereas only weak fluorescence was observed for ^{X}C–^{Y}G. It is often observed that the guanine base quenches the fluorescence of the neighboring fluorophore.[17,21,22] We found that the substitution of G in the ^{X}C–^{Y}G base pair to I in the ^{X}C–^{Y}I base pair resulted in a large increase in the fluorescence intensity. The use of I in the C-bulge probe would be effective for suppressing the quenching of the DANPH$^+$ fluorescence by the neighboring G in the C-bulge probe. The effect of the flanking mismatched base pair on the DANPH$^+$ fluorescence was quite marked. While the DANPH$^+$ fluorescence was quite weak when the base pair flanking the C-bulge was ^{X}C–^{Y}T, quite strong fluorescent was observed for the ^{X}A–^{Y}G base pair. Based on the T_m increase, DANPH$^+$ bound to the C-bulge flanking both ^{X}C–^{Y}T and ^{X}A–^{Y}G. Therefore, the DANPH$^+$ fluorescence was modulated by the flanking mismatched base pairs. It is particularly noteworthy that the guanine in the ^{X}A–^{Y}G did not quench the fluorescence of the neighboring DANPH$^+$ bound to the C-bulge. While we do not have

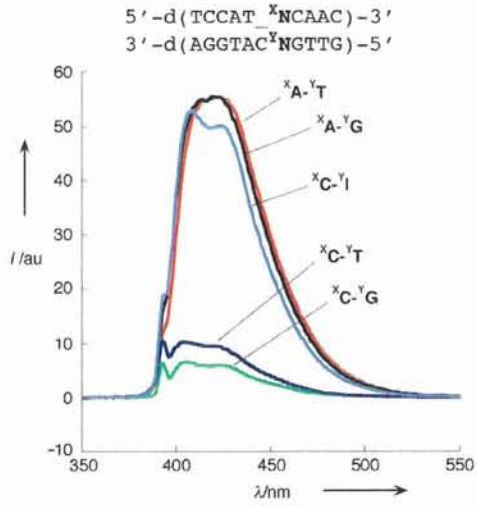

Figure 3. Fluorescence spectra of DANP (10 μM) was measured in the presence of C-bulge duplexes (50 μM) in a phosphate buffer (pH 7.0) and NaCl (100 mM). Excitation wavelength was 394 nm. ^{X}N–^{Y}N = A—T (red), A—G (black), C—T (blue), C–G (green), C—I (sky blue).

a rational explanation for these observations at this moment, this fluorescent property of DANPH$^+$ is worthy of future investigations.

Encouraged by the fluorescent measurements on selected matched and mismatched base pairs flanking the C-bulge, we have looked at the comprehensive survey of the effect of the flanking base pairs on the DANPH$^+$ fluorescence. Because the assay conditions with an excess amount of DNA are not feasible in practical SNP typing, the fluorescence measurements of DANPH$^+$ were investigated in the presence of a limited amount of C-bulge duplex. Since the absorption and emission spectra of the DANPH$^+$–C-bulge complex was shifted by 30 nm to a longer wavelength compared with those of unbound DANP, it was anticipated that we could selectively monitor the DANPH$^+$ bound to the C-bulge in the presence of unbound DANP. The DANPH$^+$ fluorescence was measured with 410 nm excitation and 460 nm emission filters to selectively monitor the DANPH$^+$ -bound complex in the presence of unbound DANP (λ_{max} 365 nm). The observed fluorescence intensity (I_{obs}) in the presence of the C-bulge duplex is reported as a value (I_{rel}) relative to that of the background (I_{back}) measured without the C-bulge duplex.

There were two sequence motifs for the C-bulge probe in terms of the relative position of the C-bulge to the ^{X}N–^{Y}N base pair. The sequences 5′-A_^{X}N-3′/3′-TC^{Y}N-5′, 5′-T_^{X}N-3′/3′-AC^{Y}N-5′, and 5′-C_^{X}N-3′/3′-IC^{Y}N-5′ contained the bulged cytosine at the 3′ end of ^{Y}N, whereas other three sequences 5′-^{X}N_A-3′/3′-^{Y}NCT-5′, 5′-^{X}N_T-3′/3′-^{Y}NCA-5′, and 5′-^{X}N_C-3′/3′-^{Y}NCI-5′ contained the bulged cytosine at the 5′ end of ^{Y}N. The 5′-G_^{X}N-3′/3′-CC^{Y}N-5′ and 5′-^{X}N_G-3′/3′-^{Y}NCC-5′ sequence contained G at the 5′ or 3′ end of ^{X}N produced the I_{rel} to be 1 regardless to the ^{X}N–^{Y}N base pair and are not discussed here. The G flanking C-bulge in the probe was replaced with inosine to avoid fluorescence quenching by G.

The C-bulge in the first sequence series showed a common tendency of I_{rel} as representatively described for 5′-A_^{X}N-3′/3′-TC^{Y}N-5′(Table 2). Among 20 C-bulges in the sequence series of 5′-A_^{X}N-3′/3′-TC^{Y}N-5′, six C-bulges flanking ^{X}T–^{Y}A, ^{X}A–^{Y}A, ^{X}A–^{Y}T, ^{X}A–^{Y}G, ^{X}A–^{Y}I, and ^{X}C–^{Y}I showed the I_{rel} larger than 2. The largest I_{rel} was 4.2 for the

Table 2. I_{rel} of DANPH$^+$ bound to the C-bulge in the A_^{X}N/TC^{Y}N sequence.[a]

	5′-d(ACATCCAA_^{X}NCAACCAC)-3′ 3′-d(TGTAGGTTC^{Y}NGTTGGTG)-5′			
^{Y}N	^{X}N			
	T	A	G	C
^{Y}A	2.8	2.5	1.0	1.5
^{Y}T	1.4	3.5	0.9	1.2
^{Y}C	1.1	1.4	1.0	1.0
^{Y}G	1.4	3.1[b]	1.0	1.3
^{Y}I	1.9	4.2	1.1	2.8

[a] Fluorescence measurements were carried out for the solution containing 2 μM each of two C-bulge duplex and 50 μM DANP in a phosphate buffer (pH 7.0) and 100 mM NaCl. $I_{rel} = I_{obs}/I_{back}$. The error (s.e.m.) was 0.1 for three independent measurements unless otherwise noted. [b] The error was 0.2.

C-bulge flanking ^{X}A–^{Y}I. When the ^{X}N was guanine, the I_{rel} was nearly 1 regardless to the ^{Y}N. It was also characteristic that the I_{rel} was below 1.5 for the C-bulge containing C at either ^{X}N or ^{Y}N position. The only exception was the C-bulge flanking to ^{X}C–^{Y}I. The ^{X}A–^{Y}G mismatch produced a large I_{rel}. The data clearly show that the flanking sequence to the C-bulge had considerable effects on the DANPH$^+$ fluorescence bound to the C-bulge. Other two sequences 5′-T_^{X}N-3′/3′-AC^{Y}N-5′ (Table 3), and 5′-C_^{X}N-3′/3′-IC^{Y}N-5′ (Table 4) showed the similar I_{rel} values for a given ^{X}N–^{Y}N base pair.

Table 3. I_{rel} of DANPH$^+$ bound to the C-bulge in the T_^{X}N/AC^{Y}N sequence.[a]

	5′-d(ACATCCAT_^{X}NCAACCAC)-3′ 3′-d(TGTAGGTAC^{Y}NGTTGGTG)-5′			
^{Y}N	^{X}N			
	T	A	G	C
^{Y}A	2.6	2.6	0.9	1.3
^{Y}T	1.6	4.0	0.9	1.0
^{Y}C	1.2	1.5	0.9	1.0
^{Y}G	1.1	2.7	0.9	1.0
^{Y}I	2.1	3.7	1.0	2.3

[a] See Table 2.

In the second sequence series, where C-bulge was located at the 5′ end of the ^{Y}N, the I_{rel} was also sensitive to the flanking base pairs (Tables 5–7). When ^{X}N was G, the I_{rel} was almost 1 regardless to ^{Y}N as observed in the first sequence context. In contrast, the I_{rel} for the C-bulges containing ^{X}C was about two times higher than that observed in the first sequence context. This flanking base-pair dependency of the I_{rel} was common for the second sequence context. On

Table 4. I_{rel} of DANPH$^+$ bound to the C-bulge in the C_^{X}N/IC^{Y}N sequence.[a]

	5′-d(ACATCCAC_^{X}NCAACCAC)-3′ 3′-d(TGTAGGTIC^{Y}NGTTGGTG)-5′			
^{Y}N	^{X}N			
	T	A	G	C
^{Y}A	2.3	2.2	0.9	1.2
^{Y}T	1.5	3.3	0.9	1.2
^{Y}C	1.1	1.3	0.9	1.0
^{Y}G	1.2	3.0	0.9	1.0
^{Y}I	2.1	4.2	1.0	2.4

[a] See Table 2.

Table 5. I_{rel} of DANPH$^+$ bound to the C-bulge in the ^{X}N_A/^{Y}NCT sequence.[a]

	5′-d(ACATCCA^{X}N_ACAACCAC)-3′ 3′-d(TGTAGGT^{Y}NCTGTTGGTG)-5′			
^{Y}N	^{X}N			
	T	A	G	C
^{Y}A	4.0	3.0	1.0	1.9
^{Y}T	2.6	3.5	0.9	1.8
^{Y}C	2.0	2.5	1.0	1.8
^{Y}G	1.9	2.7	0.9	1.1
^{Y}I	2.4	4.8	0.9	3.3

[a] See Table 2.

the basis of these fluorescence measurements, the fluorescence of DANPH$^+$ bound to the C-bulge was selectively modulated by the ^{X}N–^{Y}N base pair directly neighboring 5′ and 3′ sides. The G directly flanking SNP site quenched the DANPH$^+$ fluorescence and thus did not allow fluorescence measurements. There were three sequence series regarding the position of G relative to ^{X}N; ^{X}N was flanked by 1) one G at the 5′ end (5′-G^{X}NN-3′), 2) one G at the 3′ end (5′-N^{X}NG-3′), and 3) two Gs at both 5′ and 3′ end (5′-G^{X}NG-3′). In the first two sequences, fluorescence quenching by G could be circumvented by the design of C-bulge probe. Thus, the position of the C-bulge was chosen such that the C-bulge was produced at the opposite side of the G as shown in Figure 4a and b. In the third sequence, a probe

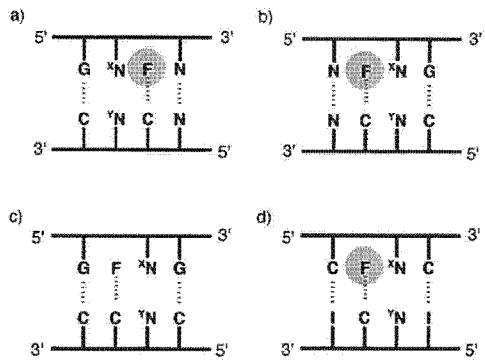

Figure 4. Discrimination of allelic types in six mutations with two C-bulge probes and DANP. Key: a) A to T; b) C to T; c) A to C; d) C to G; e) A to G; f) G to T mutations.

design was not effective to circumvent fluorescence quenching because C-bulge was always flanked by the G (Figure 4c). In this case, the fluorescence measurements should be done on the complementary strand in the 5′-C^{X}NC-3′ with the C-bulge probe having two inosine (I) opposite C (Figure 4d).

In the proposed SNP typing, the single-stranded DNA containing the SNP site was obtained by PCR followed by asymmetric PCR, then hybridized with the C-bulge probes. The DANP was added to the duplex and the fluorescence was measured. The fluorescence profiles of the given DNA sample regarding the C-bulge probes determined the SNP

Table 6. I_{rel} of DANPH$^+$ bound to the C-bulge in the ^{X}N_T/^{Y}NCA sequence.[a]

	5′-d(ACATCCA^{X}N_ACAACCAC)-3′ 3′-d(TGTAGGT^{Y}NCTGTTGGTG)-5′			
^{Y}N	^{X}N			
	T	A	G	C
^{Y}A	2.6	2.5	1.0	1.8
^{Y}T	2.3	2.8	1.0	1.9
^{Y}C	2.1	2.5	0.9	2.0
^{Y}G	1.3	1.7	0.9	1.0
^{Y}I	1.9	3.1	0.9	2.3

[a] See Table 2.

Table 7. I_{rel} of DANPH$^+$ bound to the C-bulge in the ^{X}N_C/^{X}NCI sequence.[a]

	5′-d(ACATCCA^{X}N_ACAACCAC)-3′ 3′-d(TGTAGGT^{Y}NCTGTTGGTG)-5′			
^{Y}N	^{X}N			
	T	A	G	C
^{Y}A	2.3	2.5	1.0	2.2
^{Y}T	1.9	2.8	0.9	2.3
^{Y}C	1.8	2.3	1.0	2.5
^{Y}G	1.3	1.7	0.9	1.0
^{Y}I	1.8	3.6	0.9	2.4

[a] See Table 2.

type. The SNP typing needs to discriminate three allelic types of wild type and mutant homozygotes and heterozygote. In homozygotes, the nucleotide base at the SNP site (^{X}N) is identical for two alleles, whereas a different base is found in each one of two alleles of heterozygotes. For example, in the A to C mutation, the homozygote of wild type has ^{X}A at the SNP site in two alleles (^{X}A/^{X}A), whereas the homozygote of mutant has ^{X}C in two alleles (^{X}C/^{X}C). The heterozygote has ^{X}A and ^{X}C at the SNP site in each allele (^{X}A/^{X}C). Six combinations of two bases (^{X}A/^{X}C, ^{X}A/^{X}G, ^{X}A/^{X}T, ^{X}C/^{X}G, ^{X}C/^{X}T, and ^{X}G/^{X}T) were correlated to the six types of single nucleotide mutations. The I_{rel} data shown in Tables 2–7 were obtained for the C-bulge flanked by one ^{X}N and indicated that the data were corresponding to those of homozygote samples.

The I_{rel} of heterozygote samples were measured for the DNA obtained by mixing two heterozygote samples. In Table 8, the I_{rel} data for the heterozygote samples in the 5′-A_^{X}N-3′/3′-TC^{Y}N-5′ sequence, where ^{X}N consisted of two

different nucleotide bases $^{X}N_1$ and $^{X}N_2$, is shown. The I_{rel} value was found to be the average of I_{rel} obtained for each one of two ^{X}N. This indicates that the binding of DANPH$^+$ to two different C-bulge duplexes is independent from each other under the conditions. With the I_{rel} profile of the homo- and heterozygote DNA against each one of C-bulge probes (Tables 2 and 8), the allelic type could be clearly discriminated by comparing the I_{rel} in terms of the ratio and the magnitude obtained for two C-bulge probes (Figure 5).

Table 8. I_{rel} of DANPH$^+$ bound to the C-bulge in heterozygote duplexes.[a]

	5′-d(ACATCCAA_$^{X}N_1$CAACCAC)-3′ 5′-d(ACATCCAA_$^{X}N_2$CAACCAC)-3′ 3′-d(TGTAGGTTC^{Y}NGTTGGTG)-5′ $^{X}N_1/^{X}N_2$					
^{Y}N	^{X}A/^{X}C	^{X}A/^{X}G	^{X}A/^{X}T	^{X}C/^{X}G	^{X}C/^{X}T	^{X}G/^{X}T
^{Y}A	2.0	1.7	2.6	1.2	2.1	1.9
^{Y}T	2.4	2.2	2.5	1.1	1.3	1.1
^{Y}C	1.2	1.2	1.2	1.0	1.1	1.0
^{Y}G	2.2	2.0[b]	2.3	1.1	1.3	1.2
^{Y}I	3.5[b]	2.7	3.2	2.0	2.4	1.5

[a] Fluorescence measurements were carried out for the solution containing 1 μM each of two 16 mer 5′-d(ACATCCAA$^{X}N_1$CAACCAC)-3′, 5′-d(ACATCCAA$^{X}N_2$CAACCAC)-3′ and 2 μM each of 17 mer 5′-(GTGGTTG^{Y}NCTTGGATGT)-3′ and 50 μM DANP in a phosphate buffer (pH 7.0) and 100 mM NaCl. $I_{rel}=I_{obs}/I_{back}$. The error (s.e.m.) was 0.1 for three independent measurements unless otherwise noted. [b] The error was 0.2.

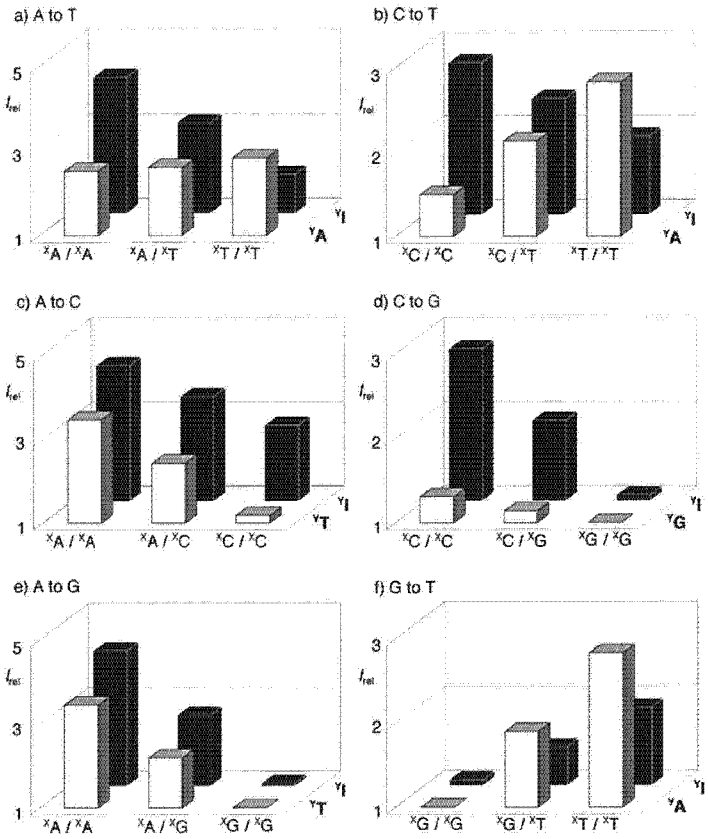

Figure 5. Selection of C-bulge probe with respect to the target sequence. a) C-bulge probe with the extra cytosine at the 5′ end of ^{Y}N; target: 5′-G^{X}NN-3′, probe: 5′-NC^{Y}NC-3′. b) C-Bulge probe with the extra cytosine at the 3′ side to ^{Y}N; target: 5′-N^{X}NG-3′, probe: 5′-C^{Y}NCN-3′. c) ^{X}N flanked by two G; target: 5′-G^{X}NG-3′, probe: 5′-C^{Y}NCC-3′. d) SNP typing should be done on the complementary strand having 5′-C^{X}NC-3′ sequence with the C-bulge contained two inosines; target: 5′-C^{X}NC-3′, probe: 5′-I^{Y}NCI-3′.

The allelic types in the A to T (or T to A) mutation were determined by two C-bulge probes containing ^{Y}A and ^{Y}I (Figure 5a). The C-bulge probe contained ^{Y}I was chosen instead of that containing ^{Y}T because the I_{rel} difference between ^{X}A and ^{X}T was larger for ^{Y}I than for ^{Y}T. Three allelic types of ^{X}A/^{X}A, ^{X}A/^{X}T, and ^{X}T/^{X}T produced a similar I_{rel} for the ^{Y}A-containing probe, but gave markedly different I_{rel} values for the ^{Y}I-containing probe. The ratio of I_{rel} obtained for the two C-bulge probes determined the allelic type. In the C to T (or T to C) and A to C (or C to A) mutations (Figure 5b and c), the allelic type could be also determined by the ratio metric analysis. The other three mutations of G to N (N = A, T, and C) could be analyzed by the difference in the intensity of I_{rel} for each of the C-bulge probes used for the analysis. Because the ^{X}G/^{X}G homozygote showed an I_{rel} of 1.0, the I_{rel} of the heterozygote (^{X}G/^{X}N) would be one half of that obtained for ^{X}N/^{X}N homozygote DNA. For a practical applicability, the predetermined profile of I_{rel} for the allelic type could be used as a standard for the diagnosis of testing samples.

Conclusion

The SNP-typing method described here exploits the C-bulge as a scaffold to recruit and keep DANP directly neighboring the SNP site. The method does not require covalent modification of the probe DNA and uses only one fluorescent molecule, that is, DANP, for the assay. The high flexibility in the probe design is another characteristic of the proposed SNP typing and makes the method applicable in principle to any target sequence. Especially, the fluorescence quenching by G could be circumvent by probe design and the effective use of inosine in the probe. However, bulge binding molecules with improved fluorescence properties, stronger fluorescence intensity, a large absorption and emission shift upon binding to C-bulge, and a large fluorescence difference with neighboring base pairs are necessary for this proposed method to be applicable for SNP typing. It is also important to understand the chemical basis that the DANPH$^+$–C bulge complex neighboring ^{X}A–^{Y}G, ^{X}C–^{Y}I and ^{X}A–^{Y}I base pairs emitted strong fluorescence. These studies may provide a way to avoid the fluorescence quenching by ^{X}G.

Experimental Section

Measurements of melting temperature of bulge-containing duplexes: DANP (50 μM) was dissolved in a sodium cacodylate (10 mM, pH 7.0) containing bulge duplex (2 μM) and NaCl (100 mM). The thermal denaturation profile was recorded on a Shimadzu UV2550 spectrometer equipped with a Shimadzu TMSPC-8 temperature controller. The absorbance of the sample was monitored at 260 nm from 4 °C to 80 °C with a sample heating rate of 1 °C min^{-1}.

UV and fluorescent spectra measurements: UV spectra were recorded on a Shimadzu UV2550 spectrometer. Fluorescent spectra were recorded on a Shimadzu RF-5300PC. DNA samples were prepared in 10 mM sodium phosphate buffer at the designated pH 7.0 in the presence of 100 mM sodium chloride. Excitation wavelength for the fluorescent measurements was the wavelength at the absorption maximum unless otherwise noted.

The fluorescence intensity was recorded on a Berthold Mithras LB 940 with 410 nm excitation and 460 nm emission filters. The measurements were carried out for the solution containing 2 μM each of two C-bulge duplex and 50 μM of DANP on the phosphate buffer (pH 7.0) and 100 mM NaCl.

Acknowledgements

This work was supported by a Grant-in-Aid for Scientific Research (C) from Japan Science for the Promotion of Science and Health and Labour Sciences Research Grants for Research on Advanced Medical Technology from the Ministry of Health, Labour and Welfare.

[1] P. Y. Kwok, *Annu. Rev. Genomics Hum. Genet.* **2001**, *2*, 235.
[2] A.-C. Syvänen, *Nat. Rev. Genet.* **2001**, *2*, 930.
[3] J. Tost, V. G. Gut, *Mass Spectrom. Rev.* **2002**, *21*, 388.
[4] T. G. Drummond, M. G. Hill, J. K. Barton, *Nat. Biotechnol.* **2003**, *21*, 1192.
[5] K. Nakatani, *ChemBioChem* **2004**, *5*, 1623.
[6] M. Strerath, A. Marx, *Angew. Chem.* **2005**, *117*, 8052; *Angew. Chem. Int. Ed.* **2005**, *44*, 7842.
[7] A. Okamoto, Y. Saito, I. Saito, *J. Photochem. Photobiol. C* **2005**, *6*, 108.
[8] A. Yamane, *Nucleic Acids Res.* **2002**, *30*, e97.
[9] G. T. Hwang, Y. J. Seo, B. H. Kim, *J. Am. Chem. Soc.* **2004**, *126*, 6528.
[10] Y. J. Seo, J. H. Ryu, B. H. Kim, *Org. Lett.* **2005**, *7*, 4931.
[11] K. Yamana, Y. Fukunaga, Y. Ohtani, S. Sato, M. Nakamura, W. J. Kim, T. Akaike, A. Maruyama, *Chem. Commun.* **2005**, 2509.
[12] O. Köhler, D. V. Jarikote, O. Seitz, *ChemBioChem* **2005**, *6*, 69.
[13] A. P. Silverman, E. T. Kool, *Nucleic Acids Res.* **2005**, *33*, 4978.
[14] L. Valis, N. Amann, H.-A. Wagenknecht, *Org. Biomol. Chem.* **2005**, *3*, 36.
[15] A. Okamoto, K. Kanatani, I. Saito, *J. Am. Chem. Soc.* **2004**, *126*, 4820.
[16] Y. Saito, Y. Miyauchi, A. Okamoto, I. Saito, *Chem. Commun.* **2004**, 1704.
[17] C. Dohno, I. Saito, *ChemBioChem* **2005**, *6*, 1075.
[18] K. Yoshimoto, C.-Y. Xu, S. Nishizawa, T. Haga, H. Satake, N. Teramae, *Chem. Commun.* **2003**, 2960.
[19] K. Yoshimoto, S. Nishizawa, M. Minagawa, N. Teramae, *J. Am. Chem. Soc.* **2003**, *125*, 8982.
[20] H. Suda, A. Kobori, J. Zhang, G. Hayashi, K. Nakatani, *Bioorg. Med. Chem.* **2005**, *13*, 4507.
[21] A. O. Crockett, C. T. Wittwer, *Anal. Biochem.* **2001**, *290*, 89.
[22] C. A. M. Seide, A. Schulz, M. H. M. Sauer, *J. Phys. Chem.* **1996**, *100*, 5541.

Received: October 20, 2006
Revised: November 30, 2006
Published online: ■■ ■■, 2007

A recruiting scaffold: The probe DNA provides a C-bulge as a scaffold to recognize and retain the fluorescent molecule DANP (*N*,*N*′-bis(3-aminopropyl)-2,7-diamino-1,8-naphthyridine, denoted as F) directly neighboring the single nucleotide polymorphism site at ^{X}N. The DANP fluorescent probe was selectively modulated by the flanking ^{X}N–^{Y}N base pair, thus reporting the type of mutation.

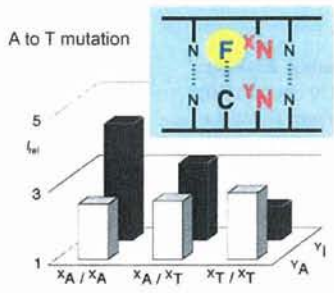

DNA Base Pairing

*F. Takei, H. Suda, M. Hagihara, J. Zhang, A. Kobori, K. Nakatani** ..... ■■■■–■■■■

Allele Specific C-Bulge Probes with One Unique Fluorescent Molecule Discriminate the Single Nucleotide Polymorphism in DNA

Anal. Chem. **2007**, *79*, 2552–2555

Exploiting Small Molecule Binding to DNA for the Detection of Single-Nucleotide Mismatches and Their Base Environment

Xiaohong Li,† Haifeng Song,† Kazuhiko Nakatani,‡ and Heinz-Bernhard Kraatz*,†

Department of Chemistry, University of Saskatchewan, 110 Science Place, Saskatoon, Saskatchewan, S7N 5C9, Canada, and Department of Regulatory Bioorganic Chemistry, The Institute of Scientific and Industrial Research (SANKEN), Osaka University, Ibaraki 567-0047, Japan

Naphthyridine–azaquinolone (Npt–Azq, described previously by Nakatani et al. (Nakatani, K.; Hagihara, S.; Goto, Y.; Kobori, A.; Hagihara, M.; Hayashi, G.; Kyo, M.; Nomura, M.; Mishima, M.; Kojima, C. *Nat. Chem. Biol.* 2005, *1*, 39–43.), was exploited to detect an adenine–adenine mismatch with a symmetrical G–C flanking sequence (5′-GAC-3′/5′-CAG-3′) in a synthetic 20-mer DNA by electrochemical impedance spectroscopy. This innovative strategy enables us to obtain information about the presence of a specific mismatch in addition to sequence information. Npt–Azq binds the G–A region of the mismatch, which causes significant changes in the structure of the DNA, which in turn causes changes in the electrochemical properties of DNA/Npt–Azq films. For a 20-mer DNA containing an A–A mismatch, the electron-transfer resistance (R_{CT}) of the system is significantly different in the presence of bound Npt–Azq, presumably due to the structural differences in the two films. Npt–Azq does not bind to matched DNA, and thus, the presence of Npt–Azq does not affect the electrochemical properties of such films.

Charge transport through DNA is sensitive to slight variation in the base pair π-stacking,[1–3] DNA sequence, and its structure.[4] Monitoring charge transport has allowed the development of a series of sensitive assays for the detection of base-stack perturbations, including mismatches.[1–3] Electrochemical mismatch detection often relies on the presence of probe molecules. Intercalators, such as daunomycin[1] and methylene blue,[2] chemically attached molecules, such as ferrocene,[5] and solution-based probes such as $[Fe(CN)_6]^{3-/4-}$ [6] have been employed.

Optical methods also have made significant contributions for the detection of mismatches.[7–15] Recently, the small molecular ligand, naphthyridine-azaquinolone (Npt–Azq) was employed to detect guanine–adenine (G–A) mismatches by surface plasmon resonance.[16] It was shown that Npt–Azq strongly interacts with G–A through hydrogen bonding and that the region flanking the mismatch is crucial for the molecular recognition. On the basis of this binding ability, Npt–Azq was used to study $(CAG)_n$ trinucleotide repeats.[17] It was shown that two Npt–Azq molecules can bind to a A–A mismatch and to the neighboring 3′-Gs in the CAG/CAG sequence. The two bases bind with one Npt–Azq molecule through complementary hydrogen bonding. As a result, a cytidine (C) nucleotide was induced to extrude from the hairpin structure. Thus, base pair π-stacking is strongly influenced, causing a large chiral change in the DNA duplex, which manifests itself in the CD spectrum of the duplex. As a result, one may expect that the electronic properties of the DNA will change too. It is important to point out that this molecule provides more than just information about the presence of a particular mismatch. In essence it also provides some information about the immediate base pair environment of the mismatch and thus gives sequence information. There are of course a large number of reports available dealing with the sequence-specific interactions of small

* To whom correspondence should be addressed. E-mail: kraatz@skyway.usask.ca.

† University of Saskatchewan.

‡ Osaka University.

(1) Kelley, S. O.; Boon, E. M.; Barton, J. K.; Jackson, N. M.; Hill, M. G. *Nucleic Acids Res.* **1999**, *27*, 4830–4837.
(2) Boon, E. M.; Ceres, D. M.; Drummond, T. G.; Hill, M. G.; Barton, J. K. *Nat. Biotechnol.* **2000**, *18*, 1096–1100.
(3) Boal, A. K.; Barton, J. K. *Bioconjugate Chem.* **2005**, *16*, 312–321
(4) Shao, F.; Augustyn, K.; Barton, J. K. *J. Am. Chem. Soc.* **2005**, *127*, 17445–17452.
(5) Yu, C. J.; Wan, Y. J.; Yowanto, H.; Li, J.; Tao, C. L.; James, M. D.; Tan, C. L.; Blackburn, G. F.; Meade, T. J. *J. Am. Chem. Soc.* **2001**, *123*, 11155–11161.
(6) Li, X. H.; Zhou, Y. L.; Sutherland, T. C.; Baker, B.; Lee, J. S.; Kraatz, H. B. *Anal. Chem.* **2005**, *77*, 5766–5769.
(7) Skogerboe, K. J. *Anal. Chem.* **1995**, *67*, 449R–454R.
(8) Wagner, R.; Debbie, P.; Radman, M. *Nucleic Acids Res.* **1995**, *11*, 3944–3948.
(9) Jain, K. K. *Science* **2001**, *294*, 621–623
(10) Afanassiev, V.; Hanemann, V.; Wolfi, S. *Nucleic Acids Res.* **2000**, *28*, e66.
(11) Proundnikov, D.; Timofeev, E.; Mirzabekov, A. *Anal. Biochem.* **1998**, *259*, 34–41.
(12) Ferguson, J. A.; Steemers, F. J.; Walt, D. R. *Anal. Chem.* **2000**, *72*, 5618–5624.
(13) Ali, M. F.; Kirby, R.; Goodey, A. P.; Rodriguez, M. D.; Ellington, A. D.; Neikirk, D. P.; McDevitt, J. T. *Anal. Chem.* **2003**, *75*, 4732–4739.
(14) Behrensdorf, H. A.; Pignot, M.; Windhab, N.; Kappel A. *Nucleic Acids Res.* **2002**, *30*, e64.
(15) Bi, L.-J.; Zhou, Y. F.; Zhang, J.-Y.; Zhang, Z.-P.; Xie, B.; Zhang, C.-G. *Anal. Chem.* **2003**, *75*, 4113–4119.
(16) Hagihara, S.; Kumasawa, H.; Goto, Y.; Hayashi, G.; Kobori, A.; Saito, I.; Nakatani, K. *Nucleic Acids Res.* **2004**, *32*, 278–286.
(17) Nakatani, K.; Hagihara, S.; Goto, Y.; Kobori, A.; Hagihara, M.; Hayashi, G.; Kyo, M.; Nomura, M.; Mishima, M.; Kojima, C. *Nat. Chem. Biol.* **2005**, *1*, 39–43.

10.1021/ac0615504 CCC: $37.00
Published on Web 02/06/2007

Chart 1. Small Molecular Ligand: Naphthyridine–Azaquinolone (Npt–Azq)

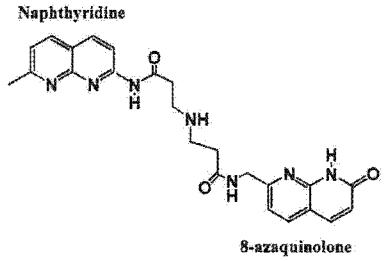

molecules with DNA. In these studies, the interaction was quantified using optical techniques.[18–20]

We set out to explore the feasibility of monitoring binding of a sequence-specific small molecule to DNA by electrochemical methods. In this study, a synthetic 20-mer DNA duplex containing a CAG/CAG unit was used to form an adenine–adenine mismatch. This mismatch is flanked by a region that allows effective binding to Npt–Azq. Electrochemical impedance spectroscopy (EIS) was used to evaluate binding of Npt–Azq to films of matched and mismatched DNA on gold. Previously we have shown that the charge-transfer resistance R_{CT} in DNA films is a useful parameter that, when compared to mismatched DNA films, allows us to determine the presence of a single-nucleotide mismatch.[6] If we can successfully detect binding of Npt–Azq to DNA, this would provide additional sequence information about the mismatch. To our knowledge, there are at present no electrochemical techniques available that provide information about the DNA sequence.

EXPERIMENTAL SECTION

Materials. Three DNA sequences were synthesized by standard solid-phase techniques using a fully automated DNA synthesizer at the Plant Biotechnology Institute (PBI-NRC, Saskatoon, SK, Canada).

1: HO-$(CH_2)_6$-SS-$(CH_2)_6$-5′-GTC-ACG-ATG-GCC-CAG-TAG-TT-3′

2: 3′-CAG-TGC-TAC-CGG-GTC-ATC-AA-5′

3: 3′-CAG-TGC-TAC-CGG-GAC-ATC-AA-5′

The characterization and purification of the DNA sequences were performed by two-step, reversed-phase HPLC and MALDI-TOF MS.

$NaClO_4$, $K_3[Fe(CN)_6]$, and $K_4[Fe(CN)_6]$ were purchased from Aldrich and used without further purification. Tris-ClO_4 were purchased from Fluka Co. Deionized water (18.2 MΩ·cm resistivity) from a Millipore Milli-Q system was used throughout this work.

N-Boc-Npt–Azq was used as reported before. The Boc group was removed by a reported procedure.[16] Prehybridized double-stranded DNA (ds-DNA) solutions (1 + 2 giving matched DNA **I** and 1 + 3 giving A–A mismatched DNA **II**) was prepared (1×10^{-4} M DNA in 50 mM Tris-ClO_4 buffer at pH 7.0). Npt–Azq was dissolved in 50 mM Tris-ClO_4 (pH 7.0, $c = 5 \times 10^{-5}$ M). This solution is then interacted with matched (**I**) or mismatched (**II**) DNA at Npt–Azq concentrations ranging from 5×10^{-5} to 5×10^{-9} M. The DNA concentration was kept constant at 1×10^{-5} M. DNA films were prepared by incubating gold microelectrodes (10 μm) for 5 days.

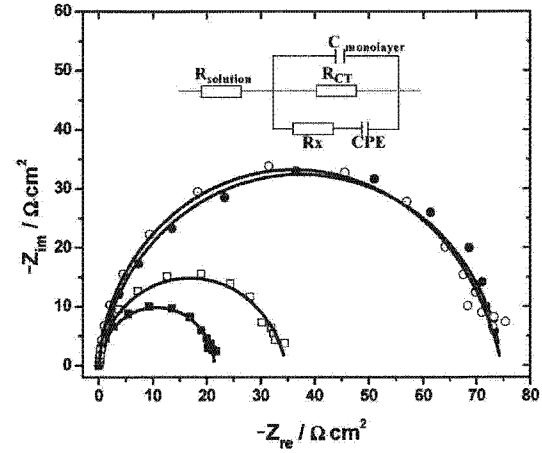

Figure 1. Typical Nyquist plots ($-Z_{im}$ vs Z_{re}) of the 20-base pair matched DNA **I** (●), **I** + Npt–Azq (○), **II** (■), and **III** (□). Measured data are shown as symbols with the fitting to the equivalent circuit as solid lines. Inset: the measured data are fit to the equivalent circuit as R_s, solution resistance; $C_{monolayer}$, capacitance of monolayer; R_{CT}, charge-transfer resistance; R_x and CPE, defects in the monolayer. The fitting data are summarized in Table 1.

Electrochemical Measurements. All measurements were carried out at room temperature (22 °C) in an enclosed and grounded Faraday cage. A conventional three-electrode system was used: a DNA modified gold microelectrode as working electrode, a Ag/AgCl/3M NaCl as reference work, and a platinum wire as counter electrode. The Ag/AgCl reference electrode, was connected to a 4 mM solution of $[Fe(CN)_6]^{3-/4-}$ in 50 mM Tris-ClO_4 buffer at pH 7.0 through a miniature salt bridge (agar plus KNO_3). EIS was measured using an EG&G 1025 frequency response analyzer interfaced to an EG&G 283 potentiostat/galvanostat. The ac voltage amplitude is 10 mV, and the voltage frequencies range from 100 kHz to 0.1 Hz. The applied potential was 250 mV versus Ag/AgCl (formal potential of the redox probe $[Fe(CN)_6]^{3-/4-}$ in the buffer solution). Importantly, all measurements were repeated for 10 electrodes to get statistically meaningful results.

RESULTS AND DISCUSSION

It has been shown that the small molecular DNA ligand, Npt–Azq, shown in Chart 1, can selectively and strongly bind to G–A through hydrogen bonding. The two parts of the molecule recognize different bases. Npt, 2-amino-1,8-naphthyridine, has three complementary hydrogen bonds that bind to G, while Azq, 8-azaquinolone, has two complementary hydrogen bonds that bind to A.[16] Solution spectroscopic studies were carried out to investigate the solution interaction of Npt–Azq with matched ds-DNA (1 + 2, **I**) and with mismatched ds-DNA (1 + 3, **II**) and are summarized in the Supporting Information (Figures S1 and S2).

(18) Dervan, Peter B. *Bioorg. Med. Chem.* **2001**, *9*, 2215–2235.
(19) Rucker, V. C.; Dunn, A. R.; Sharma, S.; Dervan, P. B.; Gray, H. B. *J. Phys. Chem. B* **2004**, *108*, 7490–7494.
(20) Kwon, Youngjoo.; Arndt, H–D.; Mao, Q.; Choi, Y.; Kawazoe, Y.; Dervan, P. B.; Uesugi, M. *J. Am. Chem. Soc.* **2004**, *126*, 15940–15941

Chart 2. Schematic Representation of the DNA Conformation Change Induced by Npt–Azq: (I) Matched DNA (strands 1 + 2), (II) A–A Mismatched DNA (strands 1 + 3), and (III) A–A Mismatched DNA (1 + 3) Binding with Npt–Azq

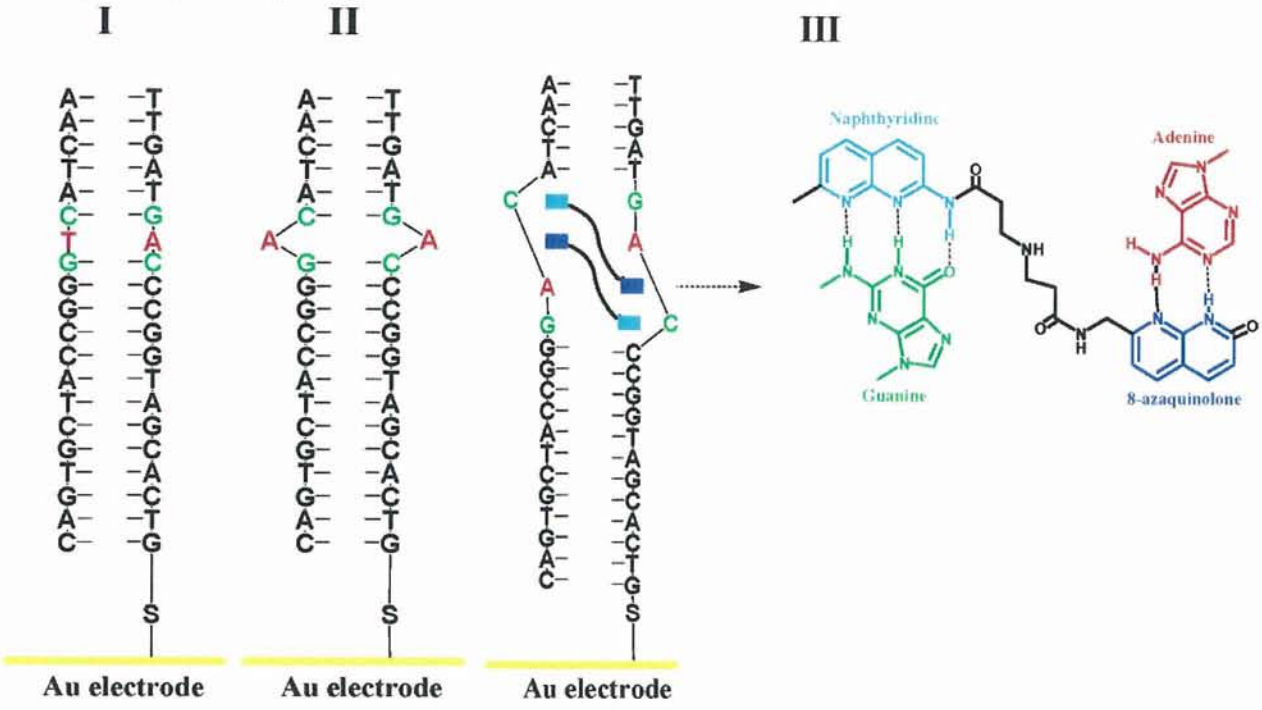

Table 1. Equivalent Circuit Element Values for DNA Films Prepared from Matched ds-DNA (I) and A–A Mismatched DNA (II) in the Presence and Absence of Npt–Azq[a]

film	R_s (Ω·cm^2)	$C_{monolayer}$ (μF cm^{-2})	R_{CT} (Ω·cm^2)	R_x (Ω·cm^2)	CPE (mF·cm^{-2})	n
I	0.01	95.5 (9.1)	74.1 (5.3)	0.1 (0.02)	3.6 (0.4)	0.8(0.02)
I + Npt–Azq	0.01	94.9 (9.1)	74.2 (5.3)	0.1 (0.02)	3.5 (0.4)	0.8(0.02)
II	0.01	105.8 (11.1)	22.0 (2.1)	0.1 (0.02)	4.5 (0.5)	0.8(0.01)
III	0.01	99.5 (9.8)	33.7 (2.9)	0.1 (0.03)	6.8 (0.7)	0.8(0.02)

[a] The values in parentheses represent the standard deviations from several electrode measurements ($n \geq 10$).

Our circular dichroism studies show that structural changes occur upon binding of Npt–Azq to mismatched DNA containing the A–A mismatch in a symmetric C–G flanking region.

Prehybridized ds-DNA was prepared as described in the Experimental Section, using matched DNA **I**, prepared by the combination of strands 1 + 2 and A–A mismatched DNA **II**, prepared by the combination of strands 1 + 3. The concentrations of the ds-DNA **I** and **II** were adjusted to 1×10^{-5} M with 50 mM Tris-ClO_4 (pH 7). Npt–Azq (5×10^{-5} M) was then added to both solutions. After incubation, DNA films were prepared on 10-μm gold electrodes exploiting the disulfide linker at the 5′-terminal side of strand 1 as shown in Chart 2. The electrochemical properties of these DNA films in the presence of $[Fe(CN)_6]^{3-/4-}$ were evaluated by EIS. Typical impedance spectra for the assembled DNA films are shown in Figure 1. These spectra are analyzed with the help of a modified Randles' equivalent circuit, as shown in the inset of Figure 1. The equivalent circuit compares well with that reported before for DNA films on 10-μm electrodes.[6]

R_s, 0.01 Ω·cm^2, is the solution resistance, which is a resistance between Ag/AgCl reference electrode and gold working electrode. $C_{monolayer}$ is used to account for DNA film capacitance. In the process of self-assembly, some defects in the films are unavoidable. The combination of R_x and a constant-phase element (CPE) accounts for possible defects in the DNA films. In addition, CPE is a nonlinear capacitor indicating inhomogeneity on the electrode surface.[21] Under our conditions, R_x (0.1 Ω·cm^2) is much smaller than R_{CT} (0.7 Ω·cm^2) for the bare electrode, which indicates that the resistance of the defect sites is small. A comparison of R_{CT} and R_x for the assembled films indicates that more homogeneous DNA films are formed on the microelectrode compared to bigger electrode (diameter, 2 mm).[22] A diffusive element that would account for the diffusion of the redox probe $[Fe(CN)_6]^{3-/4-}$ from the bulk solution to the DNA film is negligible in this system because of the absence of any Warburg impedance as shown in Figure 1.

(21) Dijkama, M.; Boukamp, B. A.; Kamp, B.; van Bennekom, W. P. *Langmuir* **2002**, *18*,3105–3112.

(22) Long, Y. T.; Li, C. Z.; Sutherland, T. C.; Kraatz, H. B.; Lee, J. S. *Anal. Chem.* **2004**, *76*, 4059–4065.

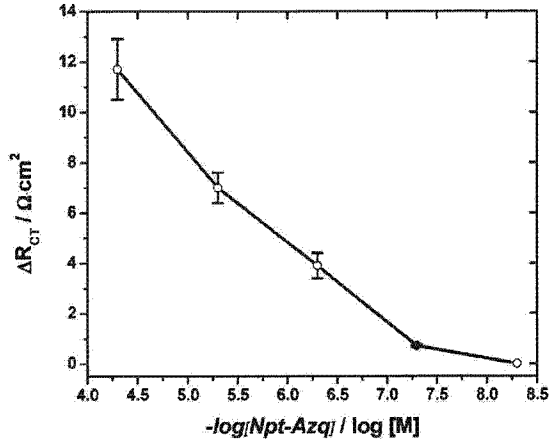

Figure 2. Relationship between ΔR_{CT} and the concentration of Npt–Azq.

The electron-transfer resistance R_{CT} is a resultant resistance accounting for the resistance of charge transfer from the $[Fe(CN)_6]^{3-/4-}$ redox probe to the electrode surface through the DNA film. For the matched ds-DNA **I**, R_{CT} is 74.1 (5.3) Ω·cm^2. For the mismatched ds-DNA **II** containing an A–A mismatch, the R_{CT} is 22.0 (2.1) Ω·cm^2. After binding of ds-DNA **II** with Npt–Azq to form the adduct **III**, R_{CT} increased to 33.7 (2.9) Ω·cm^2. Since the ligand does not bind to fully matched DNA, the addition of Npt–Azq to the matched ds-DNA **I** had no effect on the R_{CT} of the film. The explanation of the sensitivity for the mismatch in this system is provided by a simple electrostatic argument. The negatively charged $[Fe(CN)_6]^{3-/4-}$ redox probe is electrostatically repelled by negatively charged phosphates on DNA and cannot penetrate the film for a well-formed film of ds-DNA. Films that do not contain a mismatch should be better packed, while those containing a mismatch will be more disordered due to structural changes that can occur in the ds-DNA. Repulsion between the ds-DNA and the anionic redox probe is enhanced for a well-packed film; thus, R_{CT} should be higher. Following the same argument, a mismatched film containing, for example, an A–A mismatch, is presumably less tightly packed or more disordered, which allows the redox probe to penetrate the film more, resulting in a lower R_{CT}.

It is interesting to note that, after binding of Npt–Azq to a mismatched ds-DNA to form the adduct **III** as shown in Chart 2, the R_{CT} increases reproducibly from 22.0 (2.1) to 33.7 (2.9) Ω·cm^2. This suggests that the DNA film for the adduct **III** is more ordered and charge penetration is more difficult compared to films of the mismatched film of ds-DNA **II**. It is known from previous work that the Npt and Azq parts of the ligand form hydrogen bonds with guanine and adenine, respectively, showing Watson–Crick-like pairing. This will cause flipping of the cytidine out of the duplex.[17] For a mismatched film, this may in fact have dramatic consequences, making the film more rigid possibly due to the potential addition H-bonding among the flipped cytidines.

Next, we evaluated the concentration dependence. How much Npt–Azq is necessary to enable us to see an effect by EIS? In order to answer this question, we carried out dilution studies. The concentration of ds-DNA **II** was kept constant at 1×10^{-5} M, while the concentration of the ligand Npt–Azq in the solutions was varied from 5×10^{-5} to 5×10^{-9} M. As a result, films of **III** are expected to contain different amounts of Npt–Azq adducts. We monitored the difference in charge-transfer resistances ΔR_{CT} between films of the mismatched ds-DNA **II** and the adduct **III**. The relationship between ΔR_{CT} and the concentration of Npt–Azq is shown in Figure 2. We observed a virtually linear relationship between ΔR_{CT} and the concentration of Npt–Azq in the range of 5×10^{-5}–5×10^{-8} M. At a concentration of 5×10^{-9} M in Npt–Azq, there is no discernible difference between the R_{CT} for mismatched ds-DNA in the absence (**II**) and presence of the ligand Npt–Azq (**III**). Initial EIS studies of DNA films involving other mismatches (CGG/GAC and CGG/GGC) did not show significant differences in the absence and presence of Npt–Azq that would be indicative of binding.

CONCLUSION

Binding of a synthetic 20-mer DNA with the sequence-specific ligand naphthyridine–azaquinolone causes significant electrochemical effects in the ds-DNA possessing an A–A mismatch that is flanked by C–G/C–G sequences. We established the difference in the charge-transfer resistance ΔR_{CT} between films of the mismatched ds-DNA **II** and the adduct **III** as a measure that enables us to detect the bound ligand. While the ligand does not bind to matched DNA, it binds selectively to the A–A mismatched DNA **II** resulting in a ΔR_{CT} of 11. 7 (2.9) Ω·cm^2. Thus, for the first time, we were able to demonstrate the use of EIS of ds-DNA films to provide not just information about the presence of a single-nucleotide mismatch but are now able to provide base sequence information that previously was not accessible by simple electrochemical measurements.

ACKNOWLEDGMENT

This work was supported by funding through the NSERC Strategic program. H.-B.K is the Canadian Research Chair in Biomaterials. The authors also thank Don Schwab, the Plant Biotechnology Institute, Canada, for the preparation of DNA samples.

SUPPORTING INFORMATION AVAILABLE

Additional information as noted in text. This material is available free of charge via the Internet at http://pubs.acs.org.

Received for review August 18, 2006. Accepted December 19, 2006.

AC0615504

DOI: 10.1002/cbic.200600564

Small-Molecule Binding to the Nonquadruplex Form of the Human Telomeric Sequence

Yuki Goto,[a] Shinya Hagihara,[a] Masaki Hagihara,[a, b] and Kazuhiko Nakatani*[a, b]

The telomeric sequence $d(TTAGGG)_n$ located at the 3′ end of human genomic DNA plays important roles in protecting chromosomal ends from fusion, rearrangement, and translocation.[1,2] In normal cells, the entire length of the telomere gradually decreases as the replication of the genome is repeated,[3,4] due to the inability of DNA polymerase to replicate the extreme 3′ end of the template. In contrast, the enzyme telomerase is activated in the nuclei of cancer cells and maintains the length of the telomere so as to achieve immortality.[5] Therefore, ligands that bind to telomeres and inhibit their elongation are expected to be potential anticancer drugs.[6–10] The single-stranded region of the $d(TTAGGG)_n$ repeat is known to form G-quadruplex structures in vitro,[11–15] and a number of molecular ligands that bind to and strengthen the G-quadruplex structure have been investigated.[16–24]

We have taken an alternative approach to molecules binding to the telomeric sequence. Naphthyridine dimer (ND) binds to the G–G mismatch[25,26] in duplex DNA bound to the human telomeric sequence.[27] CD measurements showed that the structure of the G-quadruplex of d(AGGGTTAGGGTTAGGGTTAGGGTTA) changed upon ND binding. While we have studied the mode of ND binding to the telomeric sequence, no conclusive result was obtained, because the stoichiometry of the ND binding to the model sequence d(TTAGGGTTAGGGTTA) (telo15) of human telomere was not unique. We here report a new molecule, naphthyridine tetramer (NT), that binds to telo15 with an exclusive 1:1 binding stoichiometry. From ESI-TOF MS and UV melting profiles of telo15 mutants, it was suggested that NT bound to the two of the three G–G mismatches in the hairpin secondary structure.

NT was synthesized by a successive reductive amination of ND with glutaraldehyde. The binding of NT to the telomeric sequence, especially the binding stoichiometry, was evaluated by ESI-TOF MS (Figure 1).[28] ESI-TOF MS of telo15 showed a 4^- ion (*m/z* 1168.92) and a 3^- ion (*m/z* 1558.83) of a monomer, and a 5^- ion (*m/z* 1871.11) corresponding to a telo15 dimer, which

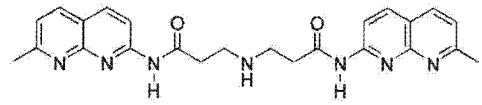

naphthyridine dimer (ND)

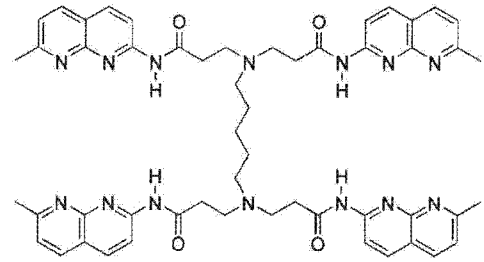

naphthyridine tetramer (NT)

was most likely an interstrand G-quadruplex. These ion peaks decreased in intensity in the presence of NT, with a concomitant appearance of a distinct ion at *m/z* 1407.71, which corresponded to the 4^- ion of a 1:1 complex of NT with telo15 ($[telo15+NT]^{4-}$). No other ions corresponding to complexes with a different binding stoichiometry or any ion of NT complexes bound to the telo15 dimer could be detected, even at a high NT concentration (60 μM). To gain an insight into the mode of NT binding to telo15, ESI-MS was performed on a mutant sequence of telo15—d(TTAZZZTTAZZZTTA) (telo15Z)—in which all of the guanine bases (G) were substituted by 7-

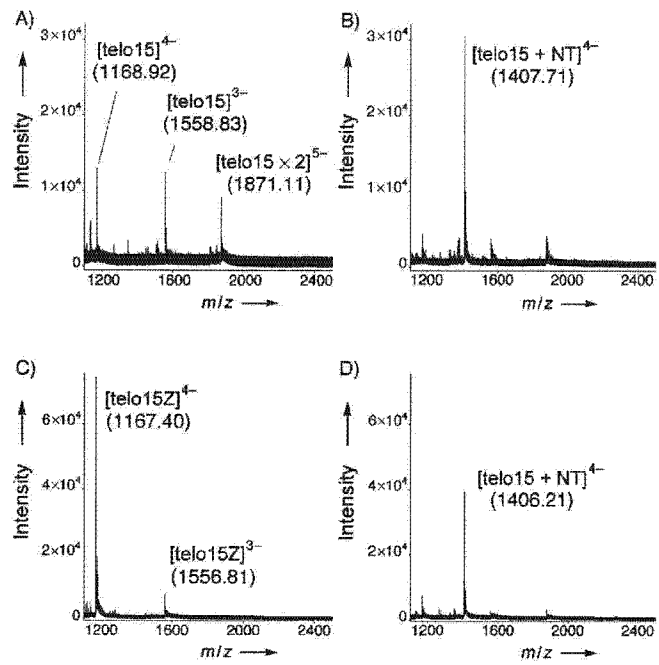

Figure 1. The ESI-TOF MS of telo15 and telo15Z with NT. The spectra were obtained in 50% aqueous methanol and 100 mM NH_4OAc. A) telo15 (20 μM), B) telo15 (20 μM) and NT (20 μM), C) telo15Z (20 μM), and D) telo15Z (20 μM) and NT (20 μM).

[a] *Y. Goto, Dr. S. Hagihara, Dr. M. Hagihara, Prof. Dr. K. Nakatani*
Department of Synthetic Chemistry and Biological Chemistry
Graduate School of Engineering, Kyoto University
Kyoto 615-8510 (Japan)

[b] *Dr. M. Hagihara, Prof. Dr. K. Nakatani*
Current address: Department of Regulatory Bioorganic Chemistry
The Institute of Scientific and Industrial Research, Osaka University
8–1 Mihogaoka, Ibaraki 567-0047 (Japan)
Fax: (+81) 6-6879-8459
E-mail: nakatani@sanken.osaka-u.ac.jp

Supporting information for this article is available on the WWW under http://www.chembiochem.org or from the author.